Bulletin of Volcanology (2026) 88:11
https://doi.org/10.1007/s00445-025-01932-y

RESEARCH ARTICLE

Switching between ordinary and non-ordinary activity at Stromboli volcano: insights from short- and long-term thermal trends recorded from space

Marco Laiolo[1,2] · Diego Coppola[1,2] · Simone Aveni[1,3] · Adele Campus[1] · Francesco Massimetti[4] · Alessandro Aiuppa[5] · Lorenzo Innocenti[6] · Giorgio Lacanna[6] · Giovanni Lo Bue Trisciuzzi[5] · Marco Pistolesi[7] · Maurizio Ripepe[6] · Marija Voloschina[7]

Received: 1 August 2025 / Accepted: 15 December 2025
© The Author(s) 2026

Abstract

Ordinary, moderately explosive activity at Stromboli is sporadically interrupted by larger effusive and explosive events that can trigger hazardous phenomena such as sector collapses, tsunamis, and ballistic fallout. We analyze 25 years of satellite infrared data to characterize the thermal pattern associated with these larger events, including: (1) effusive eruptions, (2) lava overflows, (3) major explosions, and (4) paroxysms. Increased heat flux precedes effusive eruptions and overflow sequences, and is interpreted to reflect the progressive rise of the magma column in the conduit accompanying the transition between Strombolian and effusive regimes. Conversely, major explosions are not preceded by any detectable thermal increase, although they statistically occur during periods of frequent overflows in which the Volcanic Radiative Power (VRP) is punctuated by higher values. Paroxysms (which occurred at the beginning, during and at the end of the effusive eruptions) do not show systematic thermal patterns in the preceding days, but in most cases are followed by a VRP increase. Major explosions and paroxysmal events contribute minimally to the long-term energy released by the volcano. Instead, the energy output is primarily governed by the recurrent transitions between Strombolian- and effusive-dominated regimes, sustaining a long-term, steady-state VRP of approximately 14.5 MW. Overall, only ~ 25% of the thermal energy is radiated during Strombolian activity, whereas overflows and effusions account for ~ 15% and ~ 60%, respectively. Results highlight that satellite thermal analysis is a useful tool for tracking changes of surface activity at open-vent basaltic volcanoes with frequent switching from ordinary low-energy activity to more energetic explosive or effusive eruptions.

Keywords Open-vent systems · Volcanic Radiative Power · Thermal pattern · High-energetic events · Strombolian- and effusive-dominated regimes

Introduction

Active volcanoes are geological structures that emit large amounts of thermal energy, whose intensity and persistence depend on the type of ongoing volcanic activity. Open-vent, basaltic volcanoes are characterized by a nearly continuous emission of magmatic products (magma and volcanic gases; Rose et al. 2013) and produce continuous, high-temperature thermal anomalies that can be easily detected and quantified from space (Francis et al. 1993; Glaze et al. 1989; Harris and Stevenson 1997); Oppenheimer et al. 1993a, b; Wright et al. 2002). At basaltic open-vent systems, surface activity is typically characterized by persistent gas emissions and mild explosive activity fed by a convective magma column (Kazahaya et al. 1994; Palma et al. 2011; Shinohara 2008; Stevenson and Blake 1998; Rose et al. 2013; Vergniolle and Métrich 2021; Edmonds et al. 2022). This persistent activity, often referred to as "ordinary" and characterized by low-intensity (i.e., Strombolian to Vulcanian) explosive events, typically corresponds to background (baseline) levels of monitored parameters (Newhall et al. 2017; Thompson et al. 2023; Sparks et al. 2012; Pallister and McNutt 2015; Phillipson et al. 2013).

Deviation from such ordinary activity occasionally results in more energetic events, both of explosive and effusive types (Edmonds et al. 2022; Aiuppa et al. 2021; Calvari

Editorial responsibility: N. Métrich

Extended author information available on the last page of the article

Published online: 09 January 2026

et al. 2011; Naismith et al. 2019; Ripepe et al. 2005; 2021; Shreve et al. 2019). This transition can be sudden or gradual, and its detectability by volcano monitoring networks greatly depends on the availability of long-term, homogeneous time series (Pallister and McNutt 2015; Phillipson et al. 2013; Thompson et al. 2023; Ripepe et al. 2005, 2008; Sparks et al. 2012).

Satellite thermal datasets can be particularly useful for defining baseline activity at open-vent volcanoes, since they provide multi-decadal time series of heat emission that can be acquired and elaborated in a uniform and continuous manner (Coppola et al. 2014, 2016, 2020, 2023). Thanks to their synoptic view, thermal data can greatly support monitoring activities (Coppola et al. 2022), and proved to be effective in detecting precursory signals (Thompson et al. 2023) and changes between different eruptive styles (Aiuppa et al. 2018; Barrière et al. 2022; Campion and Coppola 2023; Coppola et al. 2015, 2016; Laiolo et al. 2019; Naismith et al. 2019). Otherwise, space-based thermal data, when combined with geochemical (e.g., SO_2 flux) and geophysical (e.g., seismic tremor, deformation) data, contribute to understanding processes controlling the behavior of recurrently/persistently active volcanoes (Galetto et al. 2025; Laiolo et al. 2019; Naismith et al. 2019; Valade et al. 2016; Vasconez et al. 2022).

Stromboli volcano is an ideal laboratory for studying the transition between different activity types, since in the past decades the persistent, low-intensity explosive activity (namely the Strombolian activity) has repeatedly been punctuated by "non-ordinary" events, such as major explosions, paroxysms and lava flows of variable volume (Calvari and Nunnari 2023; Coppola et al. 2016; Laiolo et al. 2022; Ripepe et al. 2005). The processes that drive transitions from ordinary activity to more energetic explosions, and their associated timescales remain a matter of debate (Aiuppa et al. 2011, 2021; Allard 2010; Andronico and Pistolesi 2010; Métrich et al. 2021; Calvari et al. 2011; Caricchi et al. 2024; Falsaperla and Spampinato 2003; Pioli et al. 2014; Ripepe et al. 2017; Voloschina et al. 2023) since two complementary conceptual mechanisms are used to explain the driving processes. In the bottom-up mechanism, the rapid ascent from depth of gas and/or gas-rich primitive magma causes over-pressurization, hence triggering the onset of the eruptions. Conversely, in the top-down mechanisms explosions involve the decompression of the magma column, driven by the drainage of the shallower portion of the conduit due to high discharge rates during the initial phases of effusive eruptions (Ripepe et al. 2015; Calvari et al. 2011; Aiuppa et al. 2021).

Here, we analyze about 25 years of satellite thermal data elaborated by the MIROVA system (Coppola et al. 2016) to reconstruct the Volcanic Radiative Power (VRP, in Watt) emitted by Stromboli volcano between 2000 and 2024. The VRP time series is integrated with a comprehensive database of volcanic events that characterized Stromboli's activity during this period. This approach allows us to thermally characterize the ordinary (baseline) activity and to examine thermal trends before, during, and after different types of non-ordinary events. The results reveal that Stromboli's thermal activity spans nearly five orders of magnitude, providing valuable insights into persistent activity at open-vent basaltic volcanoes and highlighting deviations toward high-energetic events.

Stromboli volcano

Stromboli island represents the emerged portion (924 m above sea level) of a volcanic edifice rising approximately 3 km from the Tyrrhenian abyssal plane (Kokelar and Romagnoli 1995). The 100-ky-old subaerial volcanic edifice (Hornig-Kjarsgaard et al. 1993) has been shaped by the alternation of cycles of growth and sector collapse, both facilitated by dyke intrusions, magma upwelling and regional tectonics. The most striking geomorphological feature of the island is the Sciara del Fuoco, a horse-shoe-shaped scar representing the result of the last major sector collapse occurred at ~ 5000 yrs BP (Tibaldi 2001; Corazzato et al. 2008). The upper sector of the Sciara del Fuoco hosts the crater terrace, an oval depression oriented N40 that is divided into two main crater sectors, the NE and the SW (Massimetti et al. 2024). These two sectors host a variable number of vents feeding the Strombolian activity persistently observed for at least 2 ky (Rosi et al. 2000). This long-lasting, mild explosive activity is interpreted to be sustained by efficient magma convection and continuous recharge in the upper portion of the plumbing system, driven by degassing and crystallization of gas-richer magma supplied in near-steady state from depth (Allard et al. 1994; Harris and Stevenson 1997); Stevenson and Blake 1998). Excess degassing (Shinohara et al. 2008), a condition in which only a small fraction of degassed magma is ultimately erupted (Giberti et al. 1992; Allard et al. 1994, Harris and Stevenson 1997; Laiolo et al. 2022), is a key characteristic of Stromboli's magma budget. This background mode of activity is hereafter referred to as the "Strombolian-dominated regime", sustained by a quasi–steady-state plumbing system comprising a shallow and a deep magma reservoir. The shallow plumbing system (at ca. < 3 km depth) is occupied by the High-Porphyritic (HP), gas-poor magma erupted as black scoriae during Strombolian activity as well as during effusive episodes (Francalanci et al. 2013; Landi et al. 2009). In contrast, the deep reservoir (ca. 7–10 km depth) hosts a more primitive, gas-richer, Low Porphyritic (LP) magma. This magma is erupted as poorly crystalline, high-vesicular pumice (the so-called *golden pumices*; Francalanci et al.

2013; Métrich et al. 2001) exclusively during paroxysmal explosions and, more rarely, major explosions (Francalanci et al. 2013; Métrich et al. 2010; Voloschina et al. 2023). Although the LP magma is only ejected during explosive events of higher intensity, it is thought to continuously ascend within and resupply the shallow reservoir, producing HP magma through gas release and decompression-induced crystallization (Métrich et al. 2001, 2010).

Ordinary vs. non-ordinary events

The ordinary activity of Stromboli consists of continuous degassing and intermittent low-intensity explosions from a variable number of vents located in the two crater sectors. The Strombolian explosions occur on average every few minutes (~ 10 events/hour), ejecting small volumes of tephra (1–10 m^3) at heights typically below 200 m (see Barberi et al. 1993; Patrick et al. 2007; Ripepe et al. 2008; Rosi et al. 2013; Fig. 1a). This persistent activity is thought to be modulated by a convective magmatic column in which magma ascends, is partially erupted, and then sinks back down into the conduit (Aiuppa et al. 2010; Allard et al. 1994; 2008; Harris and Stevenson 1997; Stevenson and Blake 1998). Detailed analysis of Sentinel 2 and Landsat satellite thermal data has recently revealed that the VRP produced by this ordinary activity ranges between 1 and 30 MW and is equally partitioned between the two main crater areas, namely the north-east (NE) and south-west (SW) crater areas (Massimetti et al. 2024).

Although often considered stationary, this background activity exhibits natural fluctuations and is periodically interrupted by highly energetic events that represent a potential threat for inhabitants, visitors and for the infrastructures of the island. These events are defined here as "non-ordinary" and can be either effusive or explosive in nature (Barberi et al. 1993; Rosi et al. 2013). They have been generally classified into four main types: (i) effusive eruptions, (ii) overflows, (iii) major explosions, and (iv) paroxysmal eruptions (Fig. 1b–e).

Effusive eruptions (EE) are characterized by weekly- to monthly-long periods of continuous lava effusion from lateral vent(s) opened (at various elevations) along the Sciara del Fuoco scar. The lava flows produced during these events build important lava fields that reach the sea forming deltas (Fig. 1b) and have volumes typically in the range of 1–10 Mm^3 (Calvari and Nunnari 2023; Rosi et al. 2013). Chemically, the lavas erupted during these events correspond to degassed HP magma, similar to that erupted during ordinary activity (Landi et al. 2009).

Overflows (OF) are short-lived effusive events, characterized by the outflow of lava from the summit crater(s), with durations of few hours to several days. During these events, lava can either accumulate within the crater terrace or produce small lava flows emplaced in the upper sector of the Sciara del Fuoco depression (Fig. 1c); occasionally, the largest overflows can reach the coastline and build small lava deltas (Calvari et al. 2014; 2022; Marsella et al 2012). The volume erupted during these events is commonly less than 1 Mm^3 and often does not exceed 0.1 Mm^3 (Calvari et al. 2014).

Major explosions (ME) are intermediate-scale explosive events (Barberi et al. 1993; Métrich et al. 2005; Rosi et al. 2013) whose volume, jets duration and plume height are

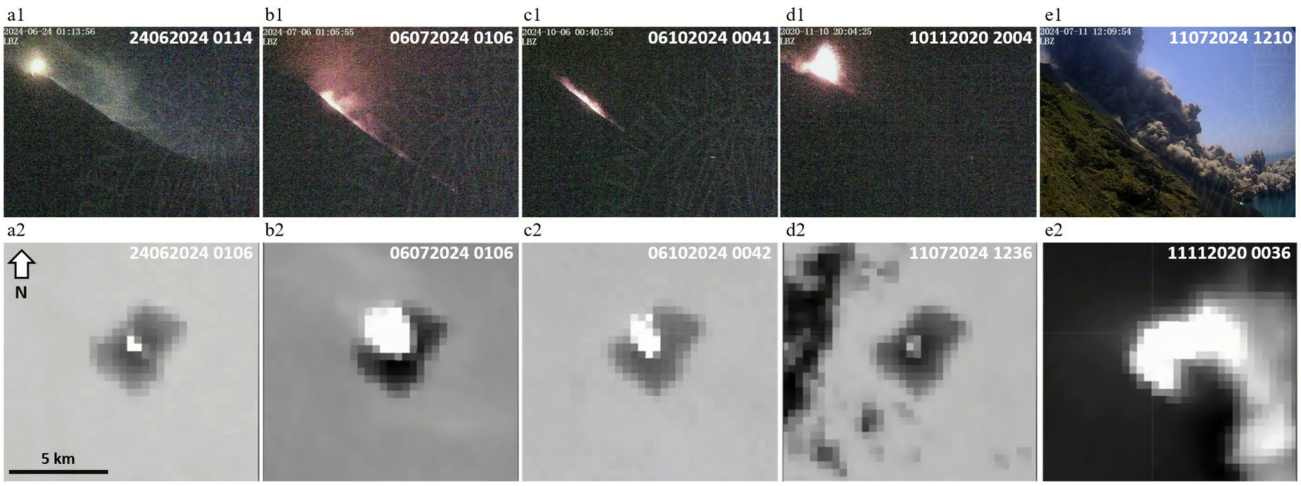

Fig. 1 **a** Mild-explosive activity from summit vent(s); **b** ongoing effusive phase of July 2024; **c** lava overflow of October 6, 2024; **d** paroxysmal explosion of July 11, 2024; **e** major explosion of Nov. 11, 2020. Optical images are captured by LBZ camera (www.lgs.unifi.it) and VIIRS-IMG (375 m. pixel resolution) acquisition in the Middle-Infrared band greyscale normalized for Brightness Temperature

intermediate between ordinary and paroxysmal explosions (Fig. 1d; Rosi et al. 2013; Voloschina et al. 2023). Major explosions generally produce ash plumes a few km in height, with tephra volumes ranging between 10^2 and 10^3 m^3 and dispersing well beyond the crater terrace (Andronico and Pistolesi 2010; Bertagnini et al. 1999; La Felice and Landi 2011; Gurioli et al. 2014; Rosi et al. 2013; Pioli et al. 2014; Voloschina et al. 2023). Intermediate melt compositions between HP and LP magmas are common to many major explosions, indicating variable degrees of interaction/homogenization between the two magmas. This suggests that the top of the deep source is activated during this type of activity, indicating intermediate depths of ca. 5–6 km b.s.l. in addition to the shallow and the deep magmatic sources (Insinga et al. 2025; Voloschina et al. 2023).

Paroxysms (P) are short-lived (minutes), violent explosive events that largely exceed, in terms of the height of the eruptive column, volume and character of the erupted materials, the ranges typical of ordinary Strombolian explosions (Fig. 1e; Rosi et al. 2013). Paroxysms generate eruptive columns up to 8 km in height, with tephra volumes from 10^4 to 10^5 m^3 (Métrich et al. 2021; Pistolesi et al. 2011; Rosi et al. 2013; Pioli et al. 2014). During these events, poorly crystalline, high-vesicular LP magma is erupted, forming the so-called *golden pumice* (Métrich et al. 2001, 2005; Francalanci et al. 2013).

Methods and dataset

Satellite thermal data

A detailed reconstruction of thermal emissions from Stromboli volcano has been obtained by merging space-based infrared data provided by:

(i) the Moderate Resolution Imaging Spectroradiometer (MODIS), onboard of TERRA and AQUA spacecrafts, launched in February 2000 and May 2002, respectively;
(ii) the Visible Infrared Imaging Radiometer Suite (VIIRS) sensors, mounted on board of NPP and JPSS-1 spacecrafts, launched in January 2012 and January 2018, respectively.

In optimal conditions, the combination of these 4 platforms allows the acquisition of up to 8 images per day of Stromboli island (4 nighttime and 4 daytime), with a spatial resolution of 0.75–1 km (Justice et al. 2002; Cao et al. 2017) in the Middle InfraRed (MIR) and Thermal InfraRed (TIR). We also use the MIR imaging band of VIIRS, which has a spatial resolution of 375 m, to enhance the detection capability of low-magnitude thermal anomalies (Coppola et al. 2022; 2023).

The full dataset, in a timespan from April 2000 and December 2024, consists of 82,329 images that have been ingested and elaborated using the MIROVA (Middle Infra-Red Observation of Volcanic Activity) algorithm, implemented for MODIS (Coppola et al. 2016) and VIIRS (Campus et al. 2022) data. Thermal anomalies are quantified using the MIR-method that allows calculating the Volcanic Radiative Power (VRP, in Watt) with an uncertainty of ± 30% and rely on the excess- and background-radiance calculation in the MIR region (Wooster et al. 2003). This parameter represents a combined measurement of the area of the volcanic emitter having an effective radiating temperature higher than 600 K sourced by the observed activity (Coppola et al. 2016; Campus et al. 2022).

The VRP time series (Fig. 2) coming from the different sensors/detectors are combined and filtered in terms of distance and/or intensity of the thermal anomaly to minimize the false alerts and the double counting (coming from different detectors acquiring at the same time) thus resulting in 9712 data points (ca. 12%; Online Resource 1). Importantly, no atmospheric correction or cloud-contamination automatic filtering is applied to the dataset. The presence of clouds in the satellite acquisitions leads, at least, to an attenuation of the thermal signal, resulting in lower retrieved VRP values compared to cloud-free images (Oppenheimer et al. 1991; Harris et al. 1998; Coppola et al. 2016). Hence, a slight underestimation of the discussed statistical parameters can be expected due to the attenuation of heat flux values caused by cloud-contaminated data. Nevertheless, here we are mainly interested in the long-term thermal trend and the overall analysis of thermal activity characterizing Stromboli in these last 25 years; therefore, when not explicitly stated (see the "Paroxysms (5 events)" section), we avoid the visual inspection of the acquired dataset to discard cloud-contaminated images.

Database of the non-ordinary events

During the period of satellite acquisitions, the ordinary Strombolian activity was repeatedly punctuated or completely interrupted by the occurrence of several effusive eruptions, overflows, major explosions and paroxysms (Fig. 2; Rosi et al. 2013; Ripepe et al. 2017; Aiuppa et al. 2021, 2025; Calvari et al. 2005; 2014; Calvari et al. 2022). To compile the database of these non-ordinary events, we rely on the official reports provided by Laboratorio of Geofisica Sperimentale (LGS; http://lgs.geo.unifi.it/) and by the National Institute of Geophysics and Volcanology (INGV; https://www.ct.ingv.it/), together with previous publications investigating Stromboli's recent activity

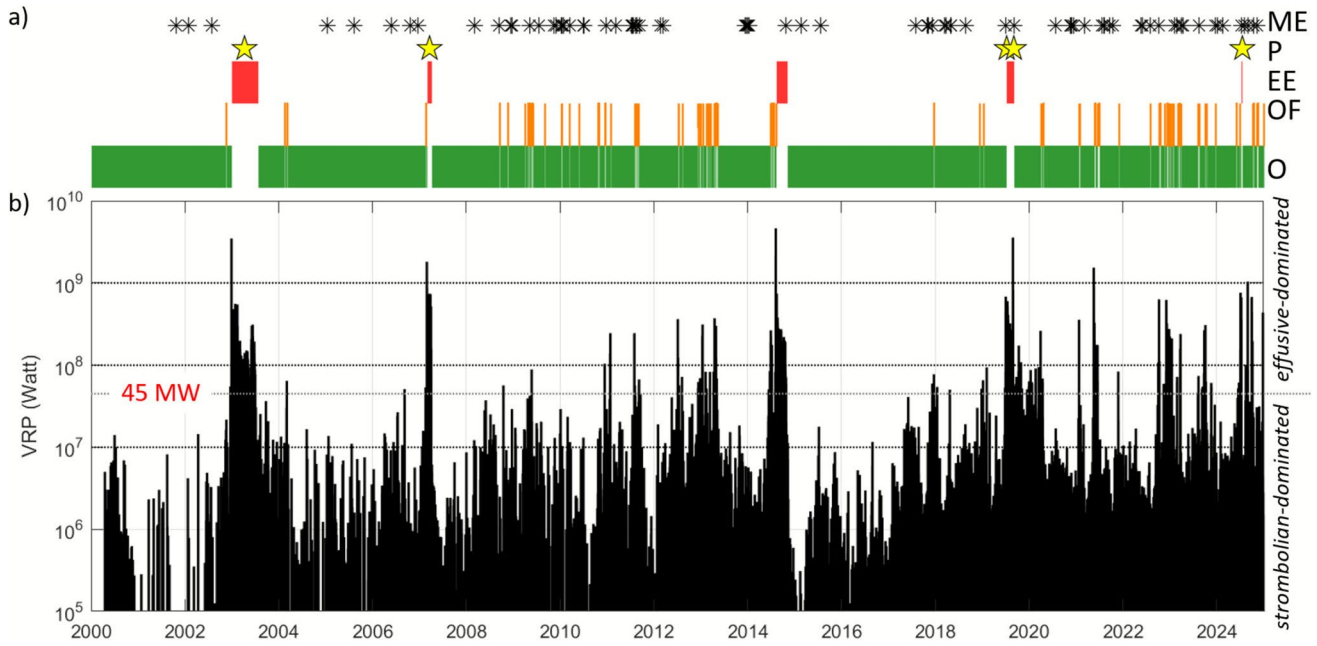

Fig. 2 **a** Daily timeline of the eruptive activity at Stromboli volcano ("O": Ordinary Strombolian activity, "OF": Overflows, "EE": Effusive Eruptions, "P": Paroxysms, "ME": Major Explosions (see the text for details); **b** time series of the Volcanic Radiative Power (VRP) from April 2000 to September 2024 at Stromboli. Dotted red line at VRP = 45 MW, show the statistically retrieved intersection value (see text for details). Dotted black lines represent the limits of each thermal level as defined in Coppola et al. (2014)

(Bevilacqua et al. 2020; Calvari et al. 2014; 2020; 2023; Rosi et al. 2013). As a result, over the 25 years of activity, we have identified:

- 5 major effusive eruptions (2002–2003, 2007, 2014, 2019 and 2024);
- 125 overflows;
- 5 paroxysms (April 5, 2003; March 15, 2007; July 3, 2019; August 28, 2019 and July 11, 2024);
- 78 major explosions.

These events are listed in Online Resource 2 where the start and end time (t_{start} and t_{end}) of each episode is reported, based on the abovementioned reports. While for effusive eruptions and some overflows, the starting and end time are very well constrained, the end time of many short-lived overflows is unknown. Of the 125 overflows analyzed, only 43 (34%) have known duration, and range from 2 h to 5 days with mean value of 24 h and median of about 13 h. Accordingly, for the remaining overflows where t_{end} was unconstrained, we set a standard duration of 24 h, which ensures the detection of any potential thermal anomaly related to these events. The total duration of major explosions and paroxysms is typically of seconds to minutes (Rosi et al. 2013). Accordingly, we set a duration of 5 min (from t_{start}) which is considered sufficient to track any thermal anomaly directly associated to the explosive events.

In the next section, the VRP dataset (April 2000–December 2024) retrieved via the MIROVA algorithm is combined with Stromboli's activity database to analyze the overall thermal signature of each activity type.

Results

Regimes and thermal levels of Stromboli's activity

The VRP time series recorded between 2000 and 2024 (Fig. 2) shows almost continuous thermal anomalies, typical of open-vent volcanoes with persistent emission of magmatic-related products. In analogy with previous work (Coppola et al. 2014, 2020; Laiolo et al. 2018; Massimetti et al. 2024), we find that the VRP produced by Stromboli volcano (log-transformed) is statistically distributed in two distinct regimes (Fig. 3a): (*i*) a low thermal regime, with mode centered at 2 MW (logVRP = 6.3), and (*ii*) high thermal regime, with modal VRP centered at 125 MW (logVRP = 8.1). The presence of these two distinct regimes is confirmed and strengthened by the fitting of our data with a Gaussian-mixture model that clearly reveals an intersection point (threshold) at 45 MW (logVRP = 7.65). The low thermal regime (VRP < 45 MW) is typically associated with continuous degassing and persistent Strombolian activity at the summit craters that we hereby define as

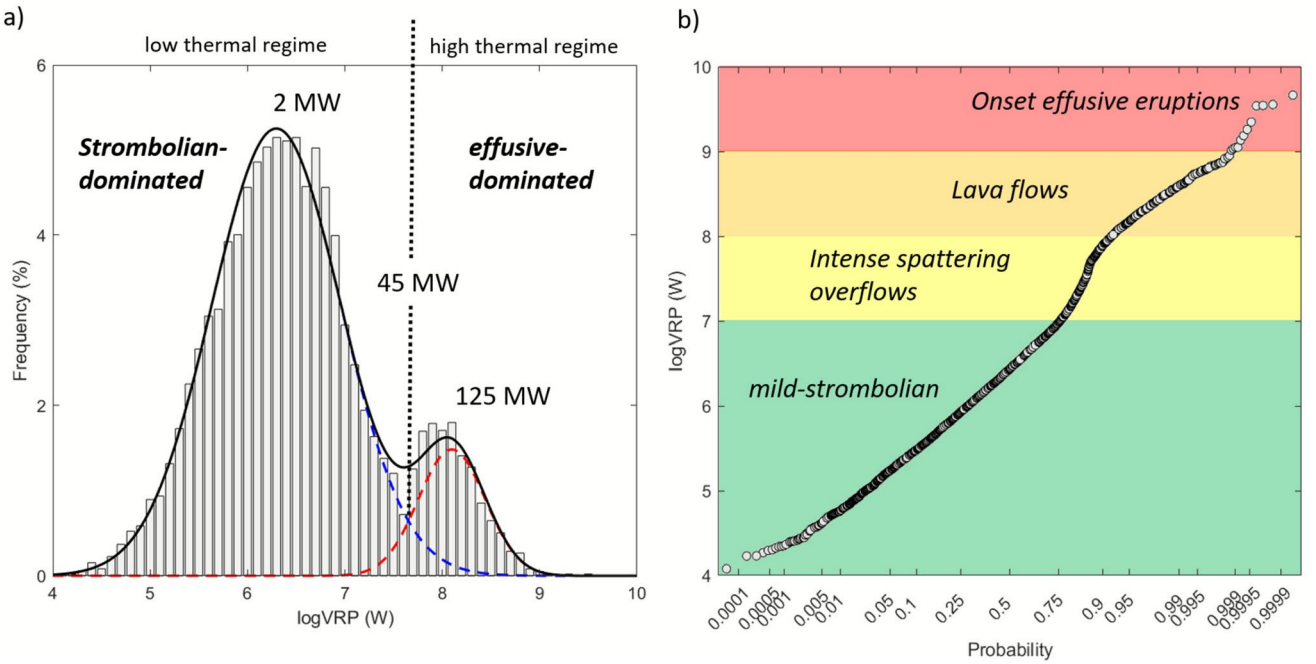

Fig. 3 **a** and **b**. Frequency histogram and probability plot of the VRP data (log-transformed) recorded in the 25 years of activity. The colors refer to the thermal levels identified by Coppola et al. (2014) to differentiate distinct activity types. The bimodal distribution is representative of two main thermal regimes (low and high) corresponding to Strombolian- and effusive-dominated heat fluxes, respectively. The transition between the two regimes occurs within the moderate thermal level ($7 < \log VRP < 8$) with an intersection value of $\log VRP = 7.6$ (45 MW)

"*Strombolian-dominated regime*" (Fig. 3a). Instead, the high thermal regime (> 45 MW) is associated with outpouring of lava flows from the summit craters or from fissures along the Sciara del Fuoco thus defining the "*effusive-dominated regime*".

A more detailed analysis of the logVRP dataset, based on the inflection points characterizing the probability distribution of the data, reveals that the two regimes can be divided into four main levels of thermal activity (Fig. 3b). We do not consider minor inflections recognized at VRP < 0.1 MW because these values are likely associated to cloud and/or to bad geometry acquisition (Coppola et al. 2014; 2016). The four levels correspond to:

- **Low thermal level (< 10 MW):** this level produces 75.3% of the anomalies and is associated with the heat flux sourced by continuous degassing and persistent Strombolian explosions occurring at one or more active vent(s) (Coppola et al. 2012, 2014; Laiolo et al. 2018; Valade et al. 2016). This low-thermal level is always associated with the Strombolian-dominated regime, which sees the heat flux controlled by the gas flux and by the level of the convective magma column (Massimetti et al. 2024).
- **Moderate thermal level (10–100 MW):** this represents 16.5% of the data and is typically associated to more vigorous Strombolian activity, intense spattering and/or to small intra-crater overflows (Coppola et al. 2014; Massimetti et al. 2024). We ascribe this level to transitional stages between the Strombolian-dominated regime (feeding the ordinary Strombolian activity) and the effusive-dominated regime,
- **High thermal level (100 MW–1 GW):** it represents 8.1% of the dataset and is associated with overflows along the Sciara del Fuoco, and more generally to lateral effusive activity (Calvari et al. 2005; Casalbore et al. 2021; Civico et al. 2021).
- **Very high thermal level (> 1 GW):** this represents only 0.13% of the data and is reached exclusively during the onset (first day) of an effusive eruption (Dec. 28, 2002; Feb. 27, 2007; Aug. 7–8, 2014), or during large-volume overflows (May 19, 2021 and Aug. 30, 2024). Notably, the only paroxysm recorded in our dataset (August 28, 2019) reached this very high level (see next section).

While the two regimes described above represent two distinct source processes of thermal activity (Strombolian- and effusive-dominated), the subdivision into four groups allows us to divide the full spectrum of VRP into stages of increasing intensity.

Syn-eruptive thermal activity of ordinary and non-ordinary events

The database in Online Resource 1 was used to calculate the statistics of syn-eruptive VRP values associated with each type of event (within the time window defined by t_{start} and t_{end}) and compare them with those of the ordinary activity (Fig. 4 and Table 1).

Unfortunately, we found no detections within the time window (5 min) of the 78 major explosions. This is not surprising since, assuming major explosions occurred randomly in time and lasted for 5 min (300 s), the probability that a single explosion overlaps with at least one satellite image over 25 years is only ~ 3% (total of 82,329 satellite images acquired, with each image capturing a 1-s frame and 4 to 8 overpasses per day). For this reason, the syn-eruptive contribution of these events remains unknown but, as suggested by ground-based parameters (seismic, infrasound and thermal camera), can be however assumed to be intermediate between mild-explosive activity and paroxysms (Calvari et al. 20210; Ripepe et al. 2021). Conversely, and by chance, one satellite acquisition occurred exactly at the climax of one of the five paroxysmal eruptions (on 28 August 2019), thus allowing us to measure its "instantaneous" VRP, although without statistical significance (see Table 1).

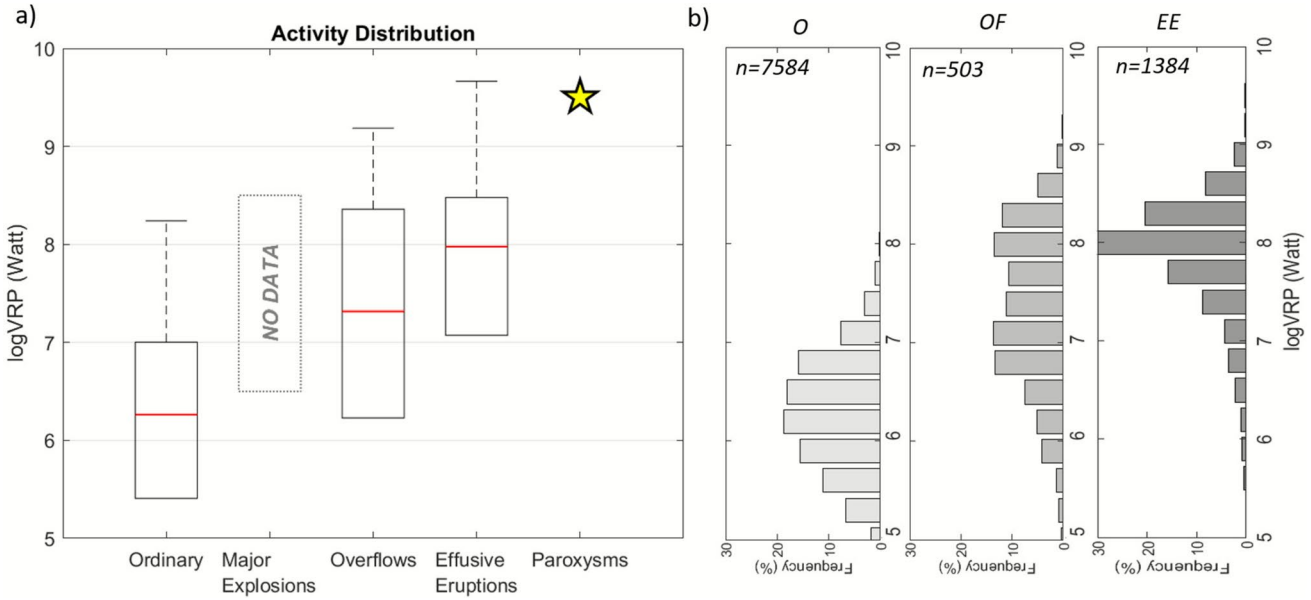

Fig. 4 **a** Box plot of logVRP data recorded during (syn-eruptive value) each activity type. **b** Syn-eruptive frequency histograms separated by activity type. Note a gradual increase in mode, mean, 90th percentile, and maximum values from ordinary activity (O) to overflows (OF) and effusive eruptions (EE). Yellow star in the boxplot represents the unique data acquired during paroxysms

Table 1 Statistics of VRP data subdivided by types of activity as described in Paragraph 2.1. The mean of SO_2 flux values obtained by UV camera since June 2014 (Delle Donne et al. 2017; Lo Bue Trisciuzzi et al. 2024). Note that a higher flux of 142 (+/− 59) t/d was measured in concomitance with the November 2009 major explosions (Insinga et al. 2025). However, these SO_2 fluxes were derived using a network of scanning spectrometers that output systematically higher values (mean: 200 ± 92 t/d), than those obtained with the UV camera system used here (see Lo Bue Trisciuzzi et al. 2024)

	Number of Data	mean VRP (MW)	percentile VRP (MW) value					mean SO_2 flux (t/d)
			10%	25%	50%	90%	100%	
Ordinary	*7584*	4.3	0.25	0.65	1.83	10.1	173.3	64
Major Explosions	-							65
Overflows	*503*	78	1.70	5.80	20.9	228.1	1536.7	100
Effusive Eruptions	*1384*	147	11.9	47.5	94.6	300.0	4617.7	177
Paroxysms	*1*						3577.0	158

Since the distributions of all types of events are influenced by data possibly attenuated by clouds, we consider the mean value, the 90th percentile and the maximum value as the most indicative parameters of the thermal emission typically associated with these events (Table 1).

Ordinary activity is characterized by a mean value of 4.3 MW, with 90th percentile thresholds close to 10 MW (Fig. 4a). These overlap the low to moderate thermal levels (< 10 MW) characterizing the Strombolian-dominated regime. Periods of extremely intense spattering or small, unreported episodes of intra-crateric overflow may be at the origin of the highest VRP (> 90th percentile), reaching a maximum value of 173 MW.

Thermal activity accompanying overflows, with an average VRP equal to 78 MW, perfectly overlaps with the moderate thermal level (10–100 MW). For these small-volumes effusive events, the 90th percentile is 228 MW and the maximum is 1537 MW, compatible with the high level (> 100 MW) range. The VRP values recorded during effusive eruptions are even higher (average, 147 MW). For the 5 main effusive eruptions, having durations of 8 to 205 days, the 90% percentile is 300 MW, while the maximum values (always recorded within the first 24 h since the beginning of an eruption) largely exceed 1 GW, compatible with the very-high level range.

Of the five paroxysms occurred at Stromboli between 2000 and 2025, only the one occurred on 28 August 2019 has been detected by our satellite data. This paroxysm occurred on 28 August 2019 at 10:17:14 UTC, during the final stages of the 2019 effusive eruption (two days before the end of lava emission). A MODIS image acquired 12 s after the onset, at 10:17:26 UTC, captured the climax of this paroxysm allowing to measure a VRP of 3577 MW (Fig. 5). Pyroclastic flows and fires occurred only a few minutes after the initial blast and therefore do not contribute to the measured VRP. Moreover, during the 48 h preceding the eruption, the effusive activity produced a VRP between 80 and 120 MW (without any observable trend; see the "Paroxysms (5 events)" section). For all these reasons, we are confident that more than 95% of the measured VRP refer to the thermal contribution of the material ejected during the explosion rather than the lava flow or other non-volcanic sources.

The paroxysm was also recorded by ground-based cameras (Andronico et al. 2021; Supplementary Movie 4) allowing a direct comparison with the satellite observation. The frame captured exactly at the time of MODIS image (Fig. 5d), suggests that the VRP was essentially produced

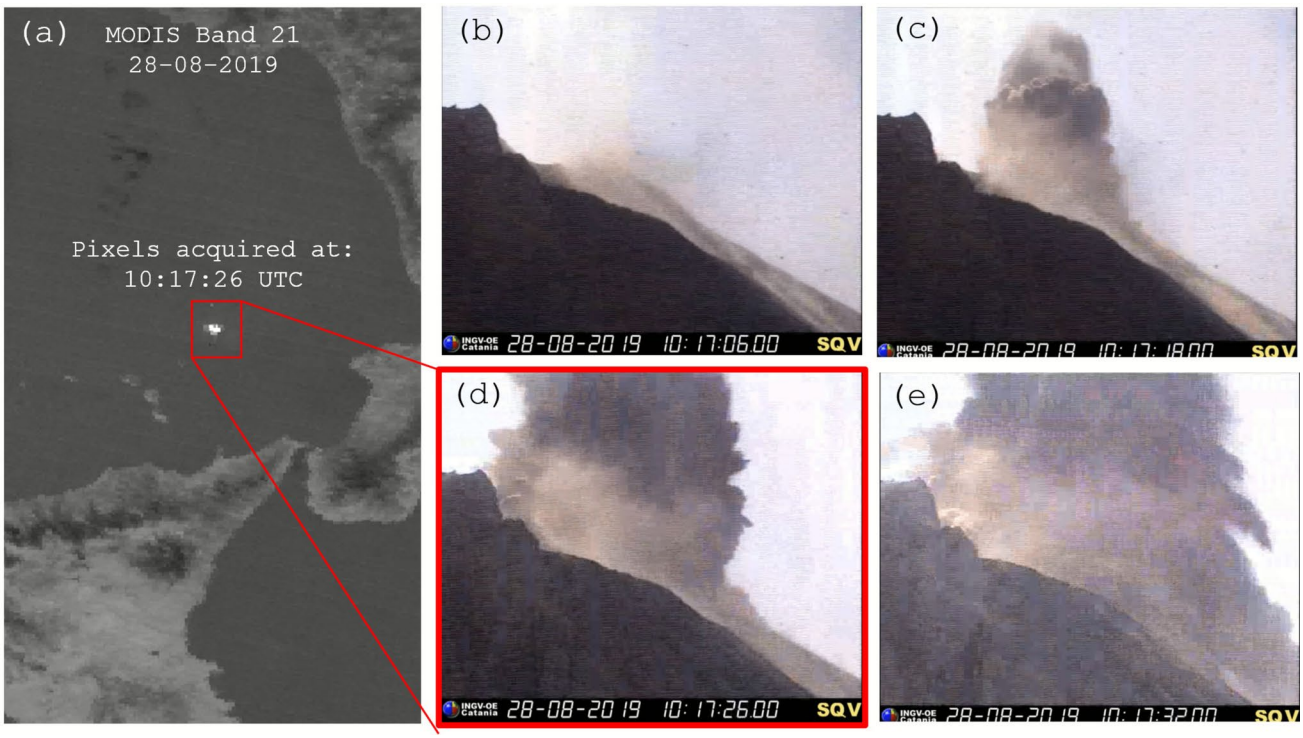

Fig. 5 **a** Snapshot of MODIS image acquired on 28 August 2019 (band 21 radiance at 3.9 microns). The bright pixels constitute the thermal anomaly detected by MIROVA and were acquired at 10:17:26 UTC. Overall, the anomaly produces a VRP of 3700 MW. **b** to **e** Four consecutive frames extracted from video acquired by the visible 400-m-high camera (Andronico et al. 2021 Supplementary Movie 4). The frame in **d** was acquired at exactly the same time of the MODIS image and displays an explosive cloud rich in incandescent fragments having a diameter of about 400 m

by the expanding explosive cloud composed by ash, lapilli and bomb-sized incandescent fragments of molten materials ejected in all directions (Andronico et al. 2021). Considering a radius of ~ 200 m (from frame analysis; Fig. 5d), we estimated that 12 s after the start of the explosion, the effective radiating temperature of the expanding cloud should have been ~ 850 K in order to produce the measured VRP (3500 MW). This is one of the highest VRP values ever recorded at Stromboli in 25 years, and is comparable to the VRP values characterizing the onset of effusive eruptions (e.g. 1700–4300 MW). We remark that two hours after the paroxysm, at 12:12 UTC, the VRP was 1118 MW, likely compatible with a reinvigorated effusive activity.

In synthesis, our results suggest that overflows, effusive eruptions and paroxysms are all characterized by VRP far higher than ordinary activity, thus supporting the notion of non-ordinary, high-energetic events (Fig. 4).

Pre-eruptive thermal trends

We analyzed the pre-eruptive phases associated with each type of volcanic activity using a time window of ± 30 days centered on the eruption onset time t_{start}. For each individual timeseries we first calculated the daily maximum VRP values. This step minimize potential underestimation due to cloud-contamination and unfavorable satellite viewing geometry geometry. Once the daily maxima were obtained, all the timeseries corresponding to the same activity type were stacked and averaged on a regular 12-h time vector spanning from t_{start} −30 days and ending at t_{start} + 30 days, to produce a representative temporal evolution of VRP (Fig. 6).

For ordinary activity, we selected 30 representative periods with length of 60 days, during which there were no reports of non-ordinary activity. We therefore consider these 30 periods as a background reference to characterize the normal variability of Strombolian activity.

Effusive eruptions (5 events)

Effusive eruptions show a clear pattern of VRP increase that rises by about one order of magnitude (from ~ 5 to ~ 50 MW) in the 2–3 weeks preceding the onset (Fig. 6a). This increase has been interpreted as a gradual rise of the magma column in response to an increased magma/gas input rate (Ripepe et al. 2005; 2015; Valade et al. 2016), the ultimate effect of this rise is the intensification of seismicity, degassing, and number of explosions before the opening of eruptive fractures (Ripepe et al. 2009; Coppola et al. 2012; Valade et al. 2016; Massimetti et al. 2024). The onset of effusive eruptions is characterized by VRP > 1 GW and is generally followed by an exponential decrease in VRP, which however can remain at high levels for days, weeks or months (Coppola et al. 2012). The initial peak and the following waning dynamics have been interpreted as the drainage of the shallow magma conduit due to the opening of lateral vents at lower elevation than the crater area (Ripepe et al. 2015; 2017).

Clustered and isolated overflows (34 events)

The analysis of stacked overflows is more complex since they can occur close together in time thus mutually influencing the pre- and post-eruptive patterns (~ 52% of the overflows take place less than 7 days after the preceding one; Online Resource 2). For this reason, we decided to focus our analysis on 34 episodes, which were preceded by at least one month of ordinary activity without the occurrence of other overflows. Moreover, we further subdivided the selected episodes into two subgroups: *(i) clustered overflows* (23 episodes) – overflows starting a sequence of additional events in which the second one does not repeat earlier than 7 days after the first and, *(ii) isolated overflows* (11 episodes) – that are single overflows followed by a return to ordinary activity.

Clustered overflows (Fig. 6b) show a pre-eruptive pattern very similar to that of effusive eruptions, with a gradual increase in VRP in the weeks preceding the onset. Here, the thermal peak at onset is lower than for effusive eruptions, with VRP between 100 and 1000 MW. The first overflow is generally followed by a sequence of clustered overflow episodes, a fact that is well consistent with the thermal flux maintaining at moderate levels for the following weeks (Fig. 6b). The similarity of the pre-eruptive trends suggests that increasing magma/gas input is the driver not only of the major flank eruptions of Stromboli, but also of periods of repeated and continuous overflows from the summit craters.

On the contrary, isolated overflows are not associated with any evident perturbation of the thermal regime, neither in the precursory nor in the post-onset phases. This suggests these events are not preceded by large variations in the magma input rate and magma column level. Rather, these isolated episodes may respond to minor transient perturbations of the shallow magmatic system (Fig. 6c). We caution however that the temporal resolution of our data (~ 12 h) does not permit to observe sudden thermal variations (a few hours long) eventually associated with rapid increase of magma flux within the shallow conduits.

Major explosions (74 events)

The analysis of the major explosions does not reveal any pre- or post-eruptive pattern, thus suggesting that these events, similarly to isolated overflows, do not disturb the thermal state of the volcano (Fig. 6d). It is therefore evident that these explosive events are not associated with a gradual rise of the magma column as occurs in clustered overflows or effusive eruptions, and do not promote successive increases

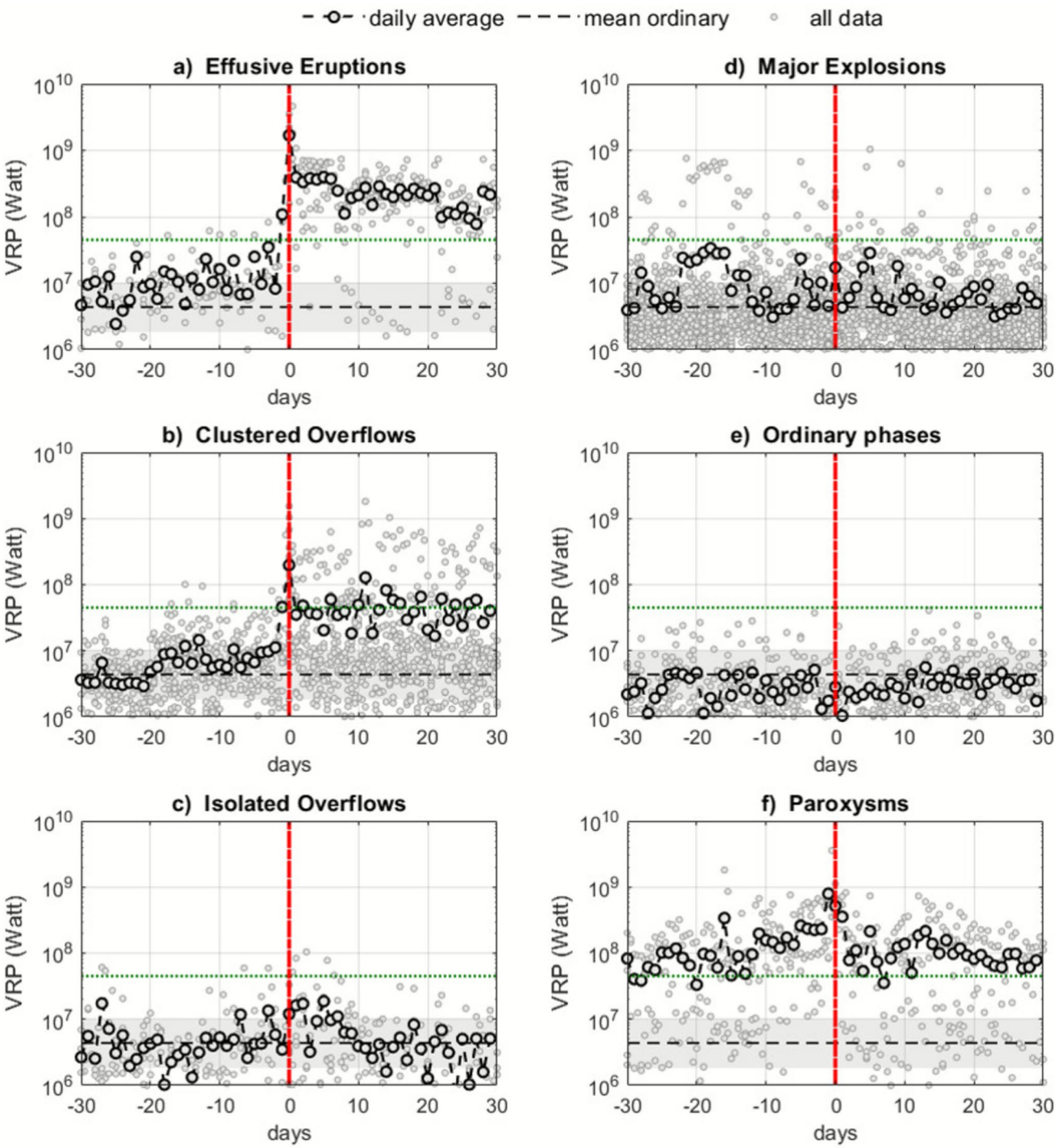

Fig. 6 Stacked VRP time series for each type of activity. Each time series is centered on the start of the events (red dashed line; see Online Resources 2) and ranges from − 30 to + 30 days. The light grey circles represent all data, while the bold black circles represent the average VRP value, calculated every 24 h. The green and black horizontal line represents, respectively, the VRP intersection value (see Fig. 3a) and the mean value of ordinary activity, with the grey field representing the 50th and 90th percentiles. See text for description of pre- and post-eruptive trends and patterns

of the activity as also evident from other monitored parameters (see LGS and INGV reports; Aiuppa et al. 2011, 2025; Voloschina et al. 2023).

Overall, the data plotted in Fig. 6d indicates that the activity before and after the major explosions is not exactly along the baseline of ordinary activity (cf. Figure 6e) but

punctuated by numerous VRP values higher than 10 MW with some higher than 100 MW. These moderate- to high-level values are related to episodes of overflows that precede, accompany or follow the ~ 38% of the major explosions considered in our analysis (cf. Online Resources 2). In this framework, we tested whether major explosions tend to occur near the timing of lava overflows, against those expected under random conditions, by comparing the observed number of explosions within varying time windows (± 1–30 days). The results show that the coupling is statistically significant for time windows lower than 14 days (p-value < 0.05), indicating that major explosions are more likely to occur within two weeks of lava overflows than expected by chance (Online Resource 3). However, the occurrence of major explosions does not perturb the thermal state of the volcano and no substantial changes are observed in the thermal pattern before and after the explosions.

Paroxysms (5 events)

Paroxysms at Stromboli have often occurred in close association with effusive eruptions (Francalanci et al. 2013; Calvari et al. 2011; Ripepe et al. 2017; Calvari and Nunnari 2023). This association has been reported frequently in the literature, although the cause of the paroxysms and their link with the effusive activity are still matter of debate (Métrich et al. 2021). The complexity also arises from the fact that the recent five paroxysms were all associated with effusive eruptions, but with very different timings and dynamics. In particular, one paroxysm (3 July 2019) marked the very beginning of a monthly-long effusive eruption, two paroxysms (5 April 2003 and 15 March 2007) occurred in the middle, while two other paroxysms (28 August 2019and 11 July 2024) occurred in the final phases of effusive activity, causing lava effusion to cease completely a few hours or a few days later. In our stacked graph (Fig. 6f), the close association between paroxysms and effusive eruptions is evident from the high thermal level characterizing the VRP before and after the events. However, the fact that each paroxysm was associated with an effusive eruption in a different way makes the analysis of stacked time series useless and subject to misinterpretation. The specific thermal pattern of each paroxysm is better revealed by taking each plot individually and filtering by visual inspection to display a more reliable trend defined exclusively by the cloud-free images (Fig. 7a–e). This analysis shows that the paroxysm of 5 April 2003, which occurred in the middle of the 2002–2003 eruption, seems to have been preceded by a decreasing trend in the week before the explosion, with a minimum recorded on 3 April (Fig. 7a). However, the limited data does not allow to understand whether this waning stage was followed by a sudden increase shortly before the explosion. The paroxysm of 15 March 2007, occurring in the middle of the eruption, also shows a decrease in VRP two days earlier (minimum on March 13), followed by 48 h of increase of the VRP (Fig. 7b).

A clear pre-explosion increasing trend is recognized before the paroxysm of 3 July 2019 (Fig. 7c), but this pattern is probably associated with the magma rising phase preceding all the effusive eruptions (cf. Figure 6a). On the contrary, the paroxysm of 28 August 2019 seems to have been preceded by a very stable VRP without highlighting any particular pattern (Fig. 7d). Finally, the last paroxysm (11 July 2024) has been preceded by a slow but gradual increase in the VRP until it reached a peak of 654 MW, a few hours before the explosion (Fig. 7e). The temporal resolution of these data does not allow to clearly reconstruct the patterns in the hours immediately preceding the paroxysms, but reveals the absence of daily-long trends common to all paroxysms. On the other hand, it seems evident that most of the paroxysms (5 April 2003, 15 March 2007, 3 July 2019; 28 August 2019) were followed by an increase in thermal activity, possibly associated with the reinvigoration of lava effusion (Fig. 7a–d). The increase appears to be persistent in some cases but temporary in others.

Long-term cumulative energies and partitioning between Strombolian- and effusive-dominated regimes

Integration of the activity database with the VRP time series allows us to estimate the contribution of each activity type to the total energy radiated by the volcano between 2000 and 2024 (Fig. 8).

We quantify the cumulative Volcanic Radiant Energy (VRE, in Joule) produced by the above-mentioned types of activity by applying the method proposed by Coppola et al. (2023). This method is based on two approaches that allow to estimate a minimum and a maximum VRE on a weekly basis and are then cumulated over the longer periods. We consider the average value between these two approaches as the most reliable, by keeping the maximum and minimum estimates as representative of the associated uncertainty (Fig. 8). Accordingly, we calculate that the recent (last 24 years) Stromboli's activity (all types of activities) radiated a total of $11.3 \pm 3.4 \times 10^{15}$ J, with a long-term, time averaged VRP of ~ 14.5 MW (Fig. 8a).

The Strombolian-dominated regime accounts for 93% of the time interval but contributes only ~ 25% of the total energy, producing $2.8 \pm 0.8 \times 10^{15}$ J, with a time averaged VRP of ~ 3.5 MW (Fig. 8b). The remaining ~ 75% of energy is radiated by the effusive-dominated regime ($8.5 \pm 2.6 \times 10^{15}$ J; Fig. 8a), and in particular by the 5 main effusive eruptions ($6.8 \pm 2.0 \times 10^{15}$ J), that concur to produce 60% of the total output (Fig. 8c). Notably, the energy of these eruptions was released on only 392 cumulative days

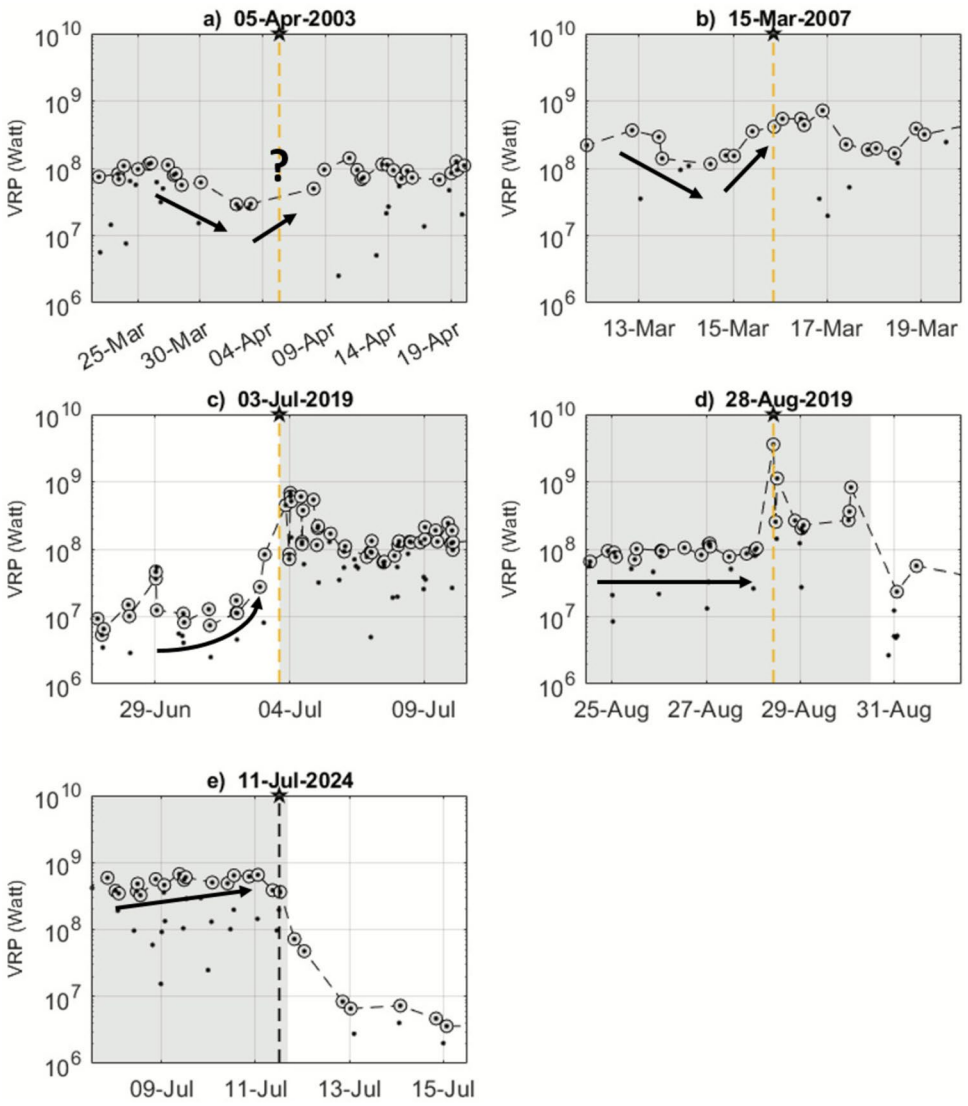

Fig. 7 Thermal trends recorded around the five paroxysms occurred between 2003 and 2024. Plots are centered on the time of the paroxysms (dashed line with star) showing data in a proper time window for each event. Shaded gray areas represent periods of lava effusions associated with the main effusive eruption. Black dots are all the data; grey circles represent the selected data after visual inspection

(~4.3% of the total analyzed period of 9132 days), producing the stepwise pattern of the cumulative VRE (Fig. 8c), characterized by a time averaged VRP of ~9.0 MW. On the other hand, the 125 overflows irradiated $1.7 \pm 0.5 \times 10^{15}$ J (Fig. 8d), corresponding to 15% of the total radiant energy. The time averaged VRP associated to these events is ~1.9 MW.

Unfortunately, our data do not allow direct measurements of the long-term thermal contribution of major explosions and paroxysms. However, indicative estimates can be made based on some considerations and literature data.

The maximum energy radiated by a single paroxysm can be estimated based on the VRP measured on August 28, 2019 (3500 MW) and assuming that this value represents the average for the entire duration of the event (assuming 5 min to provide an upper limit). In such a case, the total energy radiated by the paroxysm is equivalent to approximately 10^{12} J, or 4–6 orders of magnitude higher than the energy radiated by a typical Strombolian explosion (10^6–10^8 J; Delle Donne and Ripepe, 2012). Using this rough estimate as an upper limit, the 5 paroxysms that occurred between 2003 and 2024 would have radiated 5×10^{12} J into the atmosphere, a negligible value (0.05%) when compared to the 12×10^{15} produced totally by the other types of activity (Fig. 8). Similarly, to estimate the thermal contribution of a major explosion, we can assume an intermediate energy value between paroxysms and Strombolian explosions, which is approximately 10^{10} J per explosion. The 75 major explosions that occurred in 25 years of activity would have therefore produced 7.5×10^{11} J or 0.006% of the total energy.

In summary, the analysis of cumulative energies shows that the effusive-dominated regime, although sporadic and short-lived (only 7% of total duration compared to the whole analyzed period), constitutes by far the largest source (75%) of heat radiated by Stromboli. The Strombolian-dominated

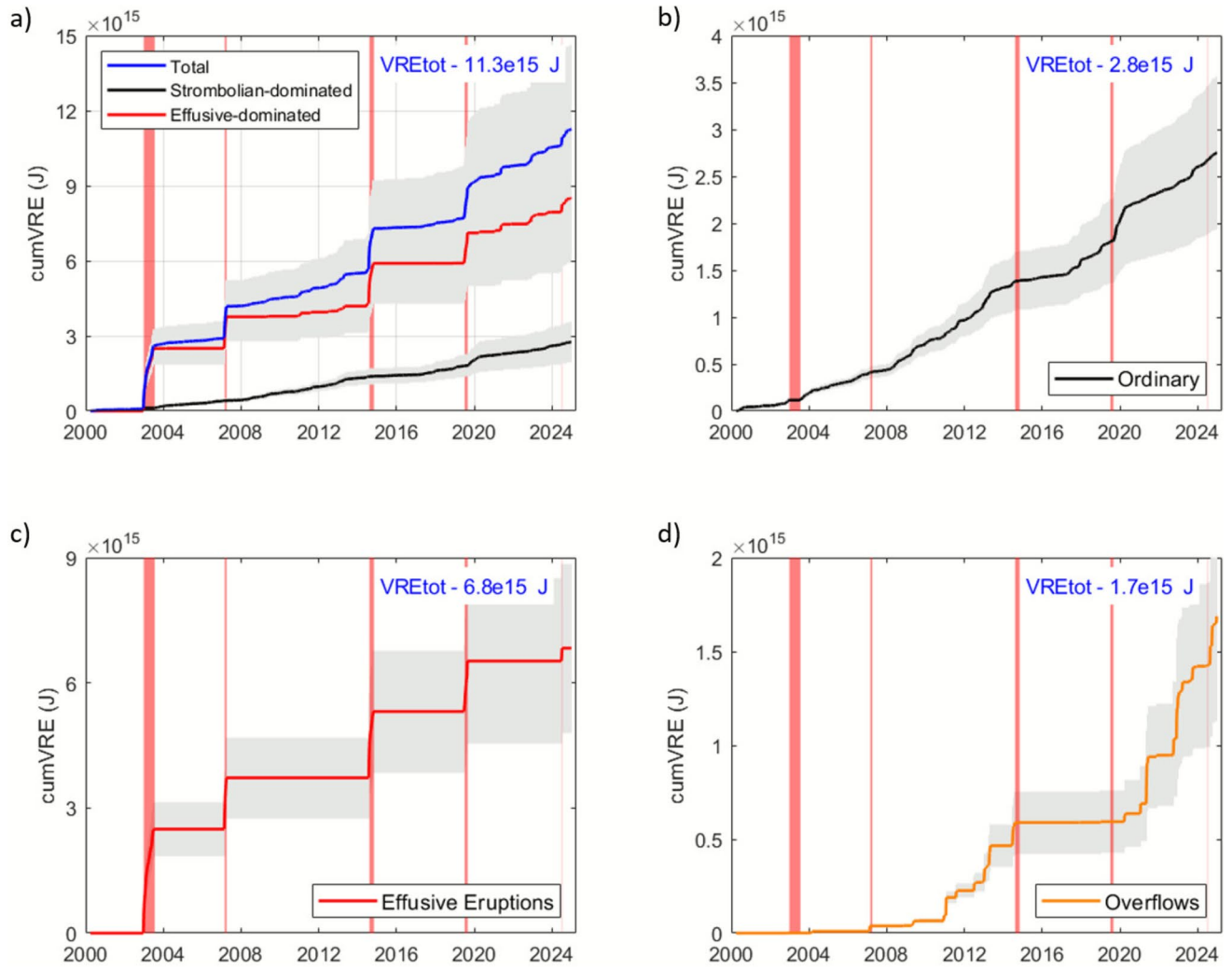

Fig. 8 Cumulative volcanic radiative energy (VRE). (**a**) total VRE and relative contributions of effusive- and strombolian-dominated regimes; (**b**) VRE produced by ordinary activity; (**c**) and (**d**) VRE produced by the 5 effusive eruptions and by overflows, respectively. The grey band indicates the error in the VRE measurement (see text for details). The vertical bars indicate the 5 effusive eruptions (Dec. 2002, Feb. 2007, Aug. 2014, Jul. 2019 and Jul. 2024)

regime concurs for the remaining 25%, while major explosions and paroxysms are essentially negligible.

Discussion

Our 25 years of continuous and homogeneous satellite records allow us to characterize the short- and long-term thermal behavior of Stromboli volcano, and to evaluate the contribution of different activity types to the total thermal budget. Here, we discuss the implications of our results for the understanding of Stromboli's thermal output during Strombolian- and effusion-dominated regimes, and for detecting the transitioning phase between the two. To support our interpretation, we also make use of published SO_2 flux results from a permanent UV Camera deployed at Stromboli since 2014 (Lo Bue Trisciuzzi et al. 2024). We use the SO_2 flux as a proxy for the time-changing rates of magma transport and degassing in the shallow (< 3 km) Stromboli's magma feeding system (Allard et al. 2008), and hence as key parameter to track the escalation in magma transport that governs the Strombolian-to-effusive transition (Delle Donne et al. 2017; Laiolo et al. 2022). In addition, thermal and SO_2 flux results are jointly analyzed in the run-up (and during) the non-ordinary explosive events.

Ultimately, we assess the potential and limitations of long-term thermal dataset and its analysis for the early detection of changes of volcanic activity and, more broadly, the possible impact on the investigation of worldwide open-vent basaltic systems.

Long-term alternation of Strombolian- and effusive-dominated regimes

Our results show that the VRP is essentially produced by two distinct source processes related to the Strombolian- and the effusive-dominated regimes, respectively. The two regimes are in turn divided into four thermal levels (low < 10 MW, medium < 100 MW, high < 1 GW and very high > 1 GW), each associated with volcanic activity types of increasing intensity (from degassing and Strombolian activity to spattering and minor overflows to major overflows and lava flows to onset of effusive eruptions; see Fig. 3b).

The Strombolian-dominated regime is characterized by continuous gas emissions and frequent Strombolian explosions (of variable intensity) sourced by one or more vents located in the crater area (Fig. 9a1). This regime is the temporally dominant activity mode of Stromboli (93% of the duration) and is characterized by VRP (~4.3 MW on average; Table 1) and SO_2 flux (64 t/d on average; Table 1; Delle Donne et al. 2017) exhibiting highly correlated temporal fluctuations (Fig. 9b). Both signals record coherent monthly-long fluctuations that support a major control played by gas on magma buoyancy, hence level of the magmatic column and ultimately VRP values. As typical for open-vent systems, in fact, increasing gas supply (i.e. SO_2) enhances magma buoyancy and convection, hence promoting the upward migration of the magma level in the conduit with consequent increase in the number of active vents and the frequency of Strombolian explosions (Ripepe et al. 2002; 2008; Massimetti et al. 2024; Shinohara 2008).

The transition between the Strombolian- and effusive-dominated regimes is systematically characterized by a gradual increase in VRP that testifies for the ascent of the magma column towards the surface to produce intense spattering and overflows (Fig. 9a2). This process is also proven by increasing SO_2 flux (reaching 100 t/d on average; Lo Bue Trisciuzzi et al. 2024; Fig. 9a2;) and by escalating seismo-acoustic activity (e.g. increasing seismic tremor, seismicity rate and acoustic pressure associated to ordinary explosive events; Ripepe et al. 2005, 2009; 2017; Valade et al. 2016).

The transition occurs within the moderate thermal level (10–100 MW; Fig. 3b), with a statistical threshold separating the two regimes of about 45 MW (Fig. 3a). As this threshold is reached, the system is prone to switch towards the effusive-dominated regime, represented by overflows from summit craters and effusive eruptions (Fig. 9a2-a3).

During the effusive-dominated phases, heat is basically sourced by the lava flow itself, with the lava output rate strongly controlling the VRP (Coppola et al. 2013). In these conditions, the VRP and the SO_2 flux may become temporarily decorrelated (Fig. 9a4, c) (Laiolo et al. 2022). The degassed (SO_2-poor) nature of the HP magma emitted during Stromboli's effusive eruptions (Burton et al. 2009; Cigolini et al. 2015; Landi et al. 2009) explains well the

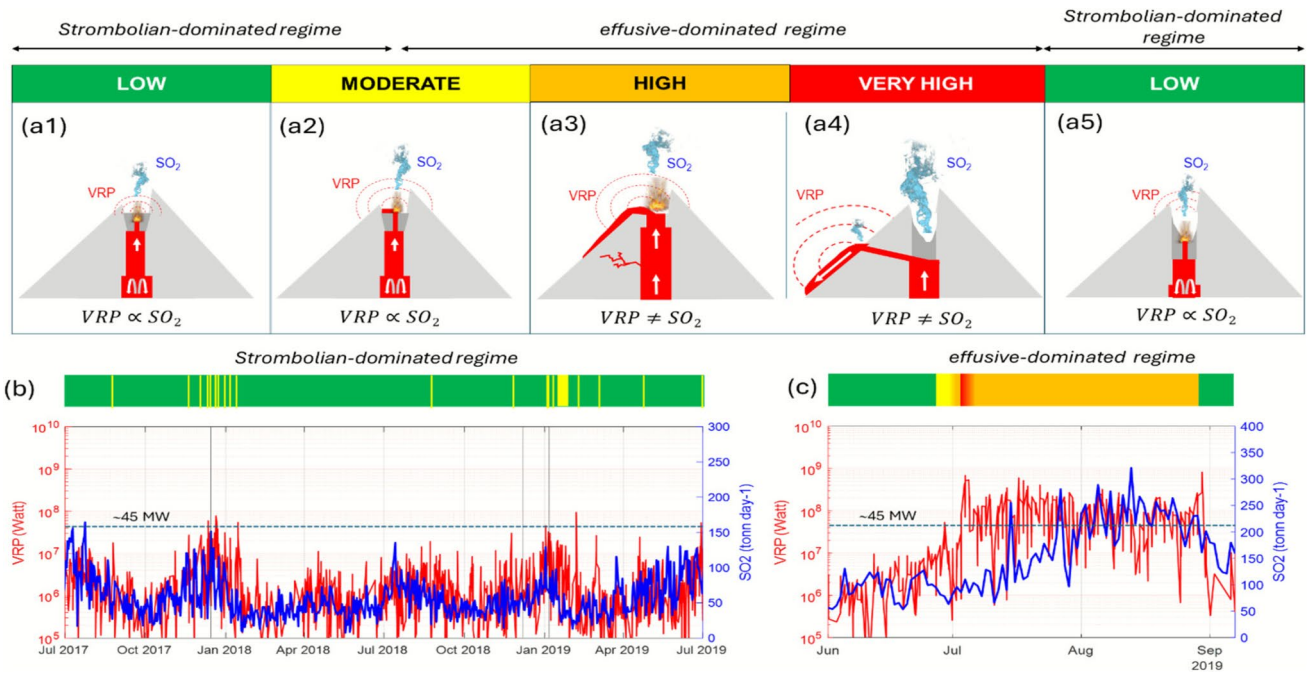

Fig. 9 **a** Conceptual sketches showing the switch between the Strombolian- and effusive-dominated regimes and back. After an effusive eruption, the lowering of the magma column brings the system back into a Strombolian-dominated regime and the cycle can begin again; **b** July 2017- June 2019 correlating trend of VRP and SO_2 flux measured at Stromboli volcano; **c** VRP and SO_2 flux decorrelation recorded during the July – August 2019 effusive eruption (see text for details)

observed decorrelation. In fact, the increase in the SO_2 emissions is less pronounced (Fig. 9c), and an unbalance may occur (Laiolo et al. 2022) when the drained lava (producing the high VRP) is not immediately balanced by new fresh (SO_2-rich) magma entering the shallow dyke/conduit feeding system (producing the SO_2 flux). This unbalance, is also testified by an abrupt drop of magma level in the conduit (Ripepe et al. 2015; 2017; Valade et al. 2016), causing the collapse of the crater area observed during all effusive eruptions. The subsequent resumption of activity will be responsible for the regrowth of the crater area through products accumulation related to the ordinary regime of the Strombolian-dominated dynamics (Fig. 9a5).

The ratio between SO_2 flux and VRP (SO_2/VRP ratio) therefore appears to be a further marker of the two distinct regimes. While in the Strombolian-dominated regime this ratio assumes values of around 15 (cf. Table 1), during the effusive regime it drops to values of around 1.2, testifying to the presence of two very distinct processes at the origin of the two signals: the fluctuation of a buoyant, convective magmatic column, in the first case, and the effusion of a degassed lava flow in the second case. These results are consistent with previous works by Laiolo et al. (2018, 2022) who interpret the transition between the two regimes as characterized by different ratios of magma input vs. magma output rate.

We thus propose that the alternation between these two regimes (i.e., Fig. 9a1-a5) is the modality through which Stromboli's shallow magmatic system maintains a decade-long steady-state behavior (cf. Harris and Stevenson 1997; Harris and Ripepe 2007), at a time-averaged VRP of ~ 14.5 MW (Fig. 8a).

Notably, the cumulative VRE curve of Stromboli resembles those of other steady-state basaltic volcanoes (e.g., Piton de la Fournaise, Kliuchevskoy, Nyamuragira before 2011, Coppola et al. 2023), which are typically characterized by closed-vent behavior (i.e., the magma conduit becomes sealed or obstructed between eruptions, leading to pressure build-up during inter-eruptive periods). In these volcanoes, a succession of discrete eruptions produces a stepwise pattern in the cumulative erupted volume; however, over longer timescales, the total erupted magma increases approximately linearly with time (Wadge et al. 1982). In the case of Stromboli, the largest steps are generated by effusive eruptions (60% of energy), while the smaller but more frequent ones are generated by overflows (15% of energy). However, unlike closed-vent volcanoes, Stromboli's inter-eruptive periods (pressure build-up stage) are characterized by a continuous heat flux generated by the ordinary activity of the Strombolian regime, which produces only 25% of the total energy.

In this steady-state alternation between the two regimes, the non-ordinary explosive events (major explosions and paroxysms) are found to play a minor role. Although they can "instantaneously" generate very high-level VRPs, comparable to effusive events (e.g. the paroxysmal eruption of August 28 generated 3500 MW, similar to the onsets of effusive eruptions), their low occurrence rate, combined with their short durations, result in cumulative energies that are overall negligible at the scale of the total thermal budget. Interestingly, the energy radiated by a single paroxysmal explosion (~ 10^{12} J) is about 4 orders of magnitude higher than the thermal energy radiated by ordinary Strombolian explosions (10^6–10^8 J; Delle Donne and Ripepe 2012), a ratio roughly consistent with the erupted tephra mass ratio characterizing these types of explosions (Métrich et al. 2021). By analogy we estimate that major explosions (energetically intermediate between Strombolian explosions and paroxysms; Métrich et al. 2010) radiate into the atmosphere 10^9–10^{10} J each.

The origin of major explosions is still debated, especially regarding the role played by either the shallow (Falsaperla and Spampinato 2003; Calvari et al. 2012) or deep (Andronico and Pistolesi 2010; Pioli et al. 2014; Voloschina et al. 2023) magmatic systems in triggering the events. Our results indicate that major explosions can occur in any active regime, whether during Strombolian or effusive, and are not preceded by systematic weekly-long trends in the VRP signal (Fig. 6). On the other hand, they tend to cluster during intervals of frequent lava overflows, suggesting a temporal connection between the two types of activity (Figs. 6d and Online Resource 3). Independent observations by Aiuppa et al. (2025) indicate that many major explosions were preceded by periods of more buoyant magma circulation (sustaining more vigorous Strombolian activity and overflows), followed by reduced SO_2 fluxes in the days/weeks before explosion. A plausible explanation is that, during phases of enhanced gas/magma supply, the magma column rises, promoting overflow activity at the surface. However, part of the gas may become temporarily trapped at depth, possibly at a structural or rheological discontinuity, leading to a reduction in SO_2 flux. The subsequent abrupt release from different depth of this accumulated gas may then trigger a major explosion or a sequence of such events (Aiuppa et al. 2025). According to this model, major explosions would reflect transient responses to perturbations that developed on larger time-scale.

Recent paroxysms have all been linked to the occurrence of effusive phases (Calvari et al. 2011; Ripepe et al. 2017; Métrich et al. 2021), although a larger dataset suggests that in the past century this was not always the case (Bevilacqua et al. 2020). Paroxysms have been thus explained in terms of either a bottom-up (Allard et al. 2010; Aiuppa et al. 2021; Métrich et al. 2021), or top- down, (Aiuppa et al. 2010, 2021; Calvari et al. 2011; Ripepe et al. 2017) mechanism, with most authors agreeing that both mechanisms can be at play. In our dataset, paroxysms show different and complex

pre-eruptive thermal trends that cannot be explained by a single mechanism. Some events appear to be preceded by a waning-waxing sequence of the VRP before the explosions (5 April 2005; 15 March 2007; Fig. 7a,b), some by extreme thermal stability (28 August 2019; Fig. 7d), and some others by a gradual VRP increase associated with processes such as (i) the gradual rise of the column during the Strombolian-dominated regime (3 July 2019; Fig. 7c) or (ii) the gradual increase of the lava output rate during the effusive-dominated regime (11 July 2024; Fig. 7e). The close connection between paroxysms and lava flows does not, however, allow us to discriminate in detail whether and how the VRP variations are linked to processes in the magma column or to more superficial processes associated with the emplacement of the lava flows.

Implications for monitoring open-vent volcanoes

The results presented here indicate that the oscillations in Strombolian activity, including the transition towards effusions, can be tracked and recognized by satellite thermal monitoring. Actually, the collection of long-lasting, homogeneous data throughout the full range of eruptive conditions occurring at persistently active volcanoes, is a fundamental requisite to recognize and discriminate background and anomalous activity (Poland et al. 2020; Philipson et al. 2013; Tilling et al. 1995).

Thanks to the availability of thermal data on a global scale (Coppola et al. 2023) the approach used in this work can be applied to other open-vent volcanoes to promptly recognize transitions between baseline activity and more energetic phenomena. Volcanoes such as Etna, Fuego, and Bezymianny (among others) all show repeated transitions in activity types and level, from baseline to paroxysmal, which can be detected with satellite thermal data (Laiolo et al. 2019; Naismith et al. 2019; Coppola et al. 2021). Similarly, lava lake level oscillations and the transition toward lateral effusive activity can be easily recognized, as already observed at Nyiragongo, Erta Ale, Kilauea, and Ambrym (Coppola et al. 2023; Coppola 2025). In all these cases, the statistical analysis of VRP, when combined with a well-constrained event timeline, offers valuable insights into the threshold values distinguishing different activity types, thereby serving as a useful tool for hazard assessment.

In terms of volcanic surveillance we must however emphasize that the identification of rapid transitions through our approach, is limited by the current temporal resolution characterizing polar-orbit constellations, that is approximately 6–12 h. This limit could be minimized by analyzing data provided by geostationary platforms (Filizzola et al. 2025 and reference therein), although their lower spatial resolution (> 1 km) reduces the capability to detect low to moderate heat flux (Ganci et al. 2012). We thus stress the importance of continuing to collect satellite data capable of providing increasingly accurate and frequent estimates of VRP and the need to combine different satellite data (with various spatial and temporal resolutions) to produce more consistent, accurate, and useful information than that provided by any individual data source.

Conclusive remarks

In this study, we analyzed 25 years of Volcanic Radiative Power (VRP) data, derived from MODIS and VIIRS satellite observations processed through the MIROVA algorithm, to characterize the long-term activity of Stromboli volcano. The VRP distribution defines two principal thermal regimes (low and high) corresponding to the Strombolian-dominated and effusive-dominated activity, respectively, with a threshold value of approximatively 45 MW. Within this framework, four distinct thermal levels were identified, each associated with a specific style of surface activity, ranging from mild-explosive events and overflows to sustained effusive eruptions, effusions onsets and paroxysms.

Stacked analysis of the thermal trends accompanying the four type of non-ordinary, high-energetic events (effusive eruptions, overflows, paroxysms and major explosions) indicate that both effusive eruptions and clusters of overflows episodes are systematically preceded by an increase in VRP, which we interpret as reflecting a progressive rise of the magma column and the transition from a Strombolian- to an effusive dominated regime. In contrast, the major explosions do not significantly alter the overall thermal output, although they are more likely to occur within two weeks of lava overflows, suggesting a temporal clustering between the two types of events. The paroxysmal eruptions exhibit more complex VRP patterns, due to their association with effusive activity. Over the entire 25-year record, Stromboli's activity alternated periodically between the two regimes. The Strombolian-dominated phase, which represent about 93% of the total duration, accounted for roughly 25% of the total $11.3 \pm 3.4 \times 10^{15}$ J radiated energy, whereas the effusive-dominated phase, lasting only 7% of the time, contributed the remaining 75%. This cyclic alternation appears to sustain the volcano's long-term steady state behavior with a time-averaged VRP of ~ 14.5 MW. Overall, our results highlight the potential of multidecadal satellite thermal datasets to identify deviations from baseline activity and to provide early insight into the onset of more energetic and hazardous eruptive phase at open-vent volcanoes.

Supplementary Information The online version contains supplementary material available at https://doi.org/10.1007/s00445-025-01932-y.

Acknowledgements MIROVA is a collaborative project between the Universities of Turin and Florence (Italy). We acknowledge the

LANCE–MODIS data system for providing MODIS and VIIRS Near Real Time products (https://nrt3.modaps.eosdis.nasa.gov/). The Authors are deeply indebted to all the individuals who, over the past 20 years, have dedicated their time, passion, and invaluable efforts to the monitoring of Stromboli volcano with instruments maintenance, data analysis and the production of over 7300 reports. The insightful discussions shared with them about the volcano's conditions have been a source of exceptional value and inspiration, profoundly enriching this work. We thank Nicole Métrich for their editorial handling of our manuscript and for their insightful comments which, together with those of Emma Nicholson and an anonymous reviewer, have greatly improved the quality of the work. The study has been developed in the framework of the service activity enhancement project "Sviluppo del sistema unico (INGV-Università) di monitoraggio vulcanico e rilevamento precoce dei maremoti e delle esplosioni parossistiche di Stromboli" funded by the Dipartimento della Protezione Civile and the INGV. The study does not necessarily reflect the policy and position of the Istituto Nazionale di Geofisica e Vulcanologia and Dipartimento della Protezione Civile, Italy.

Author contribution Marco Laiolo: Writing—original draft, Visualization, Supervision, Methodology, Investigation, Formal analysis, Data curation, Conceptualization. Diego Coppola: Writing—original draft, Visualization, Supervision, Methodology, Investigation, Formal analysis, Data curation, Conceptualization. Simone Aveni: Methodology, Investigation, Data curation. Adele Campus: Methodology, Investigation, Data curation. Francesco Massimetti: Methodology, Investigation, Data curation. Alessandro Aiuppa: Writing—review & editing, Methodology, Investigation. Lorenzo Innocenti: Methodology, Data curation. Giorgio Lacanna: Writing—review & editing, Methodology, Investigation. Giovanni Lo Bue Trisciuzzi: Methodology, Data curation. Marco Pistolesi: Writing—review & editing, Methodology, Investigation. Maurizio Ripepe: Writing—review & editing, Methodology, Investigation. Marija Voloschina: Methodology, Investigation.

Funding This work has been supported by the Italian Civil Protection in the framework of the DEVNET project and developed in the ambience of the service activity enhancement project "Sviluppo del sistema unico (INGV-Università) di monitoraggio vulcanico e rilevamento precoce dei maremoti e delle esplosioni parossistiche di Stromboli" funded by the Dipartimento della Protezione Civile and the INGV. Funding was also made available by the RETURN Extended Partnership funded by the European Union Next-GenerationEU (National Recovery and Resilience Plan – NRRP, Mission 4, Component 2, Investment 1.3 – D.D. 1243 2/8/2022, PE0000005) (Alessandro Aiuppa). Simone Aveni work was supported by the 'Piano Nazionale di Ripresa e Resilienza' (PNRR). Francesco Massimetti was supported by Universidad Nacional Autónoma de México (UNAM) Post-doctoral Program (POSDOC).

Data availability Data analyzed in this study are included in the Supplementary Materials. Further inquiries can be directed to the corresponding author. The Volcanic Radiative Power dataset on the base of this study is available here: https://doi.org/10.17605/OSF.IO/J5PDX.

Declarations

Conflict of interest The authors declare no competing interests.

Open Access This article is licensed under a Creative Commons Attribution 4.0 International License, which permits use, sharing, adaptation, distribution and reproduction in any medium or format, as long as you give appropriate credit to the original author(s) and the source, provide a link to the Creative Commons licence, and indicate if changes were made. The images or other third party material in this article are included in the article's Creative Commons licence, unless indicated otherwise in a credit line to the material. If material is not included in the article's Creative Commons licence and your intended use is not permitted by statutory regulation or exceeds the permitted use, you will need to obtain permission directly from the copyright holder. To view a copy of this licence, visit http://creativecommons.org/licenses/by/4.0/.

References

Aiuppa A, Bertagnini A, Métrich N, Moretti R, Di Muro A, Liuzzo M, Tamburello G (2010) A model of degassing for Stromboli volcano. Earth Planet Sci Lett 295(1–2):195–204. https://doi.org/10.1016/j.epsl.2010.03.040

Aiuppa A, Burton M, Allard P, Caltabiano T, Giudice G, Gurrieri S, Liuzzo M, Salerno G (2011) First observational evidence for the CO_2-driven origin of Stromboli's major explosions. Solid Earth 2:135–142. https://doi.org/10.5194/se-2-135

Aiuppa A, de Moor JM, Arellano S, Coppola D, Francofonte V, Galle B, Giudice G, Liuzzo M, Mendoza E, Saballos A, Tamburello G, Battaglia A, Bitetto M, Gurrieri S, Laiolo M, Mastrolia A, Moretti R (2018) Tracking formation of a lava lake from ground and space: Masaya volcano (Nicaragua), 2014–2017. Geochem Geophys Geosyst 19:496–515. https://doi.org/10.1002/2017GC007227

Aiuppa A, Bitetto M, Delle Donne D, La Monica F, Tamburello G, Coppola D, Della Schiava M, Innocenti L, Lacanna G, Laiolo M, Massimetti F, Pistolesi M, Silengo C, Ripepe M (2021) Volcanic CO2 tracks the incubation period of basaltic paroxysms. Sci Adv 7(38):eabh0191. https://doi.org/10.1126/sciadv.abh0191

Aiuppa A, Bitetto M, Curcio L, Delle Donne D, Lages J, Lo Bue Trisciuzzi G, Tamburello G, Vitale A, Cannavò F, Coltelli M, Coppola D, Innocenti L, Insinga L, Lacanna G, Laiolo M, Massimetti F, Pistolesi M, Privitera E, Ripepe M, Voloschina M, Cilluffo G (2025) Volcanic gas changes prior to Stromboli's major explosions are statistically significant. J Volcanol Geoth Res 462:108325. https://doi.org/10.1016/j.jvolgeores.2025.108325

Allard P (2010) A CO_2-rich gas trigger of explosive paroxysms at Stromboli basaltic volcano, Italy. J Volcanol Geoth Res 189:363–374. https://doi.org/10.1016/j.jvolgeores.2009.11.018

Allard P, Carbonnelle J, Métrich N, Loyer H, Zettwoog P (1994) Sulphur output and magma degassing budget of Stromboli volcano. Nature 368:326–330. https://doi.org/10.1038/368326a0

Allard P, Aiuppa A, Burton M, Caltabiano T, Federico C, Salerno G, La Spina A (2008) Crater gas emissions and the magma feeding system of Stromboli volcano. In: Calvari S, Inguaggiato S, Puglisi G, Ripepe M, Rosi M (eds) The Stromboli Volcano: an integrated study of the 2002–2003 eruption. Geophysical Monograph Series, vol 182. American Geophysical Union, pp 65–80. https://doi.org/10.1029/182GM07

Andronico D, Pistolesi M (2010) The november 2009 paroxysmal explosions at Stromboli. J Volcanol Geoth Res 196(1–2):120–125. https://doi.org/10.1016/j.jvolgeores.2010.06.005

Andronico D, Del Bello E, D'Oriano C, Landi P, Pardini F, Scarlato P, de Michieli Vitturi M, Taddeucci J, Cristaldi A, Ciancitto F, Pennacchia F, Ricci T, Valentini F (2021) Uncovering the eruptive patterns of the 2019 double paroxysm eruption crisis of Stromboli volcano. Nat Commun 12:4213. https://doi.org/10.1038/s41467-021-24420-1

Bani P, Aiuppa A, Coppola D, Carn S, Cluze D, Rose-Koga E, Medard E, Nauret F, Moussallam Y, Tari D, Bani I (2025) Magmatic volatiles control the sub-plinian basaltic eruptions at Ambae volcano. Vanuatu Comm Earth Environ 6:84. https://doi.org/10.1038/s43247-025-02018-5

Barberi F, Rosi M, Sodi A (1993) Volcanic hazard assessment at Stromboli based on review of historical data. Acta Vulcanol 3:173–187

Barrière J, d'Oreye N, Smets B, Oth A, Delhaye L, Subira J, Mashagiro N, Derauw D, Smittarello D, Muhindo Syavulisembo A, Kervyn F (2022) Intra-crater eruption dynamics at Nyiragongo (D.R. Congo), 2002–2021. J Geophys Res Solid Earth 127:e2021JB023858. https://doi.org/10.1029/2021JB023858

Bertagnini A, Coltelli M, Landi P, Pompilio M, Rosi M (1999) Violent explosions yield new insights into dynamics of Stromboli volcano. Eos Trans AGU 80(52):633–636. https://doi.org/10.1029/99EO00415

Bevilacqua A, Bertagnini A, Pompilio M, Landi P, Del Carlo P, Di Roberto A, Aspinall W, Neri A (2020) Major explosions and paroxysms at Stromboli (Italy): a new historical catalog and temporal models of occurrence with uncertainty quantification. Sci Rep 10:17357. https://doi.org/10.1038/s41598-020-74301-8

Burton MR, Caltabiano T, Murè F, Salerno G, Randazzo D (2009) SO_2 flux from Stromboli during the 2007 eruption: results from the FLAME network and traverse measurements. J Volcanol Geotherm Res 182(3–4):214–220. https://doi.org/10.1016/j.jvolgeores.2008.11.025

Calvari S, Nunnari G (2023) Statistical insights on the eruptive activity at Stromboli volcano (Italy) recorded from 1879 to 2023. Remote Sens 15:4822. https://doi.org/10.3390/rs15194822

Calvari S, Spampinato L, Lodato L, Harris AJL, Patrick MR, Dehn J (2005) Chronology and complex volcanic processes during the 2002–2003 flank eruption at Stromboli volcano (Italy) reconstructed from direct observations and surveys with a handheld thermal camera. J Geophys Res Solid Earth 110:B02201. https://doi.org/10.1029/2004JB003129

Calvari S, Spampinato L, Bonaccorso A, Oppenheimer C, Rivalta E, Boschi E (2011) Lava effusion—a slow fuse for paroxysms at Stromboli volcano? Earth Planet Sci Lett 301:317–323. https://doi.org/10.1016/j.epsl.2010.11.015

Calvari S, Bonaccorso A, Madonia P, Neri M, Liuzzo M, Salerno G, Behnke B, Caltabiano T, Cristaldi A, Giuffrida G, La Spina A, Marotta E, Ricci T, Spampinato L (2014) Major eruptive style changes induced by structural modifications of a shallow conduit system: the 2007–2012 Stromboli case. Bull Volcanol 76:841. https://doi.org/10.1007/s00445-014-0841-7

Calvari S, Di Traglia F, Ganci G, Bruno V, Ciancitto F, Di Lieto B et al (2022) Multi-parametric study of an eruptive phase comprising unrest, major explosions, crater failure, pyroclastic density currents and lava flows: Stromboli volcano, 1 December 2020–30 June 2021. Front Earth Sci 10:899635. https://doi.org/10.3389/feart.2022.899635

Campion R, Coppola D (2023) Classification of lava lakes based on their heat and SO2 emission: implications for their formation and feeding processes. Front Earth Sci. https://doi.org/10.3389/feart.2023.1040199

Campus A, Laiolo M, Massimetti F, Coppola D (2022) The transition from MODIS to VIIRS for global volcano thermal monitoring. Sensors 22(5):1713. https://doi.org/10.3390/s22051713

Cao C, Xiong X, Wolfe R, DeLuccia F, Liu Q, Blonski S, Lin G, Nishihama M, Pogorzala D, Oudrari H, Hillger D (2017) Visible Infrared Imaging Radiometer Suite (VIIRS) Sensor Data Record (SDR) User's Guide; Version 1.3. NOAA Technical Report NESDIS. NESDIS, College Park, MD, USA

Caricchi L, Montagna CP, Aiuppa A, Lages J, Tamburello G, Papale P (2024) CO_2 flushing triggers paroxysmal eruptions at open conduit basaltic volcanoes. J Geophys Res Solid Earth 129:e2023JB028486. https://doi.org/10.1029/2023JB028486

Casalbore D, Di Traglia F, Bosman A, Romagnoli C, Casagli N, Chiocci FL (2021) Submarine and subaerial morphological changes associated with the 2014 eruption at Stromboli Island. Remote Sens 13(11):2043. https://doi.org/10.3390/rs13112043

Cigolini C, Laiolo M, Coppola D (2015) Revisiting the last major eruptions at Stromboli volcano: inferences on the role of volatiles during magma storage and decompression. In: Zellmer GF, Edmonds M, Straub SM (eds) *The Role of Volatiles in the Genesis, Evolution and Eruption of Arc Magmas*. Geol Soc Lond Spec Publ 410:143–177. https://doi.org/10.1144/SP410.3

Civico R, Ricci T, Scarlato P, Andronico D, Cantarero M, Carr BB, De Beni E, Del Bello E, Johnson JB, Kueppers U, Pizzimenti L, Schmid M, Strehlow K, Taddeucci J (2021) Unoccupied aircraft systems (UASs) reveal the morphological changes at Stromboli volcano (Italy) before, between, and after the 3 July and 28 August 2019 paroxysmal eruptions. Remote Sens 13:2870. https://doi.org/10.3390/rs13152870

Coppola D, Piscopo D, Laiolo M, Cigolini C, Delle Donne D, Ripepe M (2012) Radiative heat power at Stromboli volcano during 2000–2011: twelve years of MODIS observations. J Volcanol Geoth Res 215:48–60. https://doi.org/10.1016/j.jvolgeores.2011.12.001

Coppola D, Laiolo M, Piscopo D, Cigolini C (2013) Rheological control on the radiant density of active lava flows and domes. J Volcanol Geoth Res 249:39–48. https://doi.org/10.1016/j.jvolgeores.2012.09.005

Coppola D, Laiolo M, Delle Donne D, Ripepe M, Cigolini C (2014) Hot-spot detection and characterization of Strombolian activity from MODIS infrared data. Int J Remote Sens 35(9):3403–3426. https://doi.org/10.1080/01431161.2014.903354

Coppola D, Macedo O, Ramos D, Finizola A, Delle Donne D, del Carpio J, White R, McCausland W, Centeno R, Rivera M, Apaza F, Ccallata B, Chilo W, Cigolini C, Laiolo M, Lazarte I, Machaca R, Masias P, Ortega M, Puma N, Taipe E (2015) Magma extrusion during the Ubinas 2013–2014 eruptive crisis based on satellite thermal imaging (MIROVA) and ground-based monitoring. J Volcanol Geoth Res 302:199–210. https://doi.org/10.1016/j.jvolgeores.2015.07.005

Coppola D, Laiolo M, Massimetti F, Hainzl S, Shevchenko AV, Mania R, Shapiro NM, Walter TR (2021) Thermal remote sensing reveals communication between volcanoes of the Klyuchevskoy Volcanic Group. Sci Rep. https://doi.org/10.1038/s41598-021-92542-z

Coppola D, Valade S, Masias P, Laiolo M, Massimetti F, Campus A, Aguilar R, Anccasi R, Apaza F, Ccallata B, Cigolini C, Cruz LF, Finizola A, Gonzales K, Macedo O, Miranda R, Ortega M, Paxi R, Taipe E, Valdivia D (2022) Shallow magma convection evidenced by excess degassing and thermal radiation during the dome-forming Sabancaya eruption (2012–2020). Bull Volcanol 84:16. https://doi.org/10.1007/s00445-022-01523-1

Coppola D, Cardone D, Laiolo M, Aveni S, Campus A, Massimetti F (2023) Global radiant flux from active volcanoes: the 2000–2019 MIROVA database. Front Earth Sci. https://doi.org/10.3389/feart.2023.1240107

Coppola D, Laiolo M, Cigolini C, Delle Donne D, Ripepe M (2016) Enhanced volcanic hot-spot detection using MODIS IR data: results from the MIROVA system. In: Harris AJL, De Groeve T, Garel F, Carn SA (eds) Detecting, Modelling, and Responding to Effusive Eruptions. Geol Soc Lond Spec Publ 426. https://doi.org/10.1144/SP426.5

Coppola D, Laiolo M, Cigolini C, Massimetti F, Delle Donne D, Ripepe M, Arias H, Barsotti S, Parra CB, Riky G, Cevuard S, Chigna G, Chun C, Garaebiti E, Gonzales D, Griswold J, Juarez J, Lara LE, López CM, Macedo O, Mahinda C, Ogburn SE, Prambada O, Ramon P, Ramos D, Peltier A, Saunders S, De Zeeuw - Van Dalfsen E, Varley N, William R (2020) Thermal remote sensing for global volcano monitoring: experiences

from the MIROVA system. Front Earth Sci 7:362. https://doi.org/10.3389/feart.2019.00362
Coppola D (2025) Thermal Monitoring of Volcanoes from Space. In: Spica Z, Caudron C (eds) Modern Volcano Monitoring. Advances in Volcanology. Springer, Cham. https://doi.org/10.1007/978-3-031-86841-2_11
Corazzato C, Francalanci L, Menna M, Petrone CM, Renzulli A, Tibaldi A, Vezzoli L (2008) What controls sheet intrusion in volcanoes? Structure and petrology of the Stromboli sheet complex, Italy. J Volcanol Geoth Res 173:26–54. https://doi.org/10.1016/j.jvolgeores.2008.01.006
Delle Donne D, Ripepe M (2012) High-frame rate thermal imagery of Strombolian explosions: implications for explosive and infrasonic source dynamics. J Geophys Res Solid Earth 117:B09311. https://doi.org/10.1029/2011JB008987
Delle Donne D, Tamburello G, Aiuppa A, Bitetto M, Lacanna G, D'Aleo R, Ripepe M (2017) Exploring the explosive-effusive transition using permanent ultraviolet cameras. J Geophys Res Solid Earth 122: 4377–4394. https://doi:10.1002/2017JB014027.
Edmonds M, Liu E, Cashman KV (2022) Open-vent volcanoes fueled by depth-integrated magma degassing. Bull Volcanol 84:3. https://doi.org/10.1007/s00445-021-01522-8
Falsaperla S, Spampinato L (2003) Seismic insight into explosive paroxysms at Stromboli volcano. Italy. J Volcanol Geotherm Res 125(1–2):137–150. https://doi.org/10.1016/S0377-0273(03)00093-3
Filizzola C, Mazzeo G, Marchese F, Pietrapertosa C, Pergola N (2025) The contribution of Meteosat third generation-flexible combined imager (MTG-FCI) observations to the monitoring of thermal volcanic activity: the Mount Etna (Italy) February–March 2025 eruption. Remote Sens 17(12):2102. https://doi.org/10.3390/rs17122102
Francalanci L, Lucchi F, Keller J, De Astis G, Tranne CA (2013) Eruptive, volcano-tectonic and magmatic history of the Stromboli volcano (north-eastern Aeolian archipelago). In: Lucchi F, Peccerillo A, Keller J, Tranne CA, Rossi PL (eds) The Aeolian Islands Volcanoes. Geol Soc Lond Mem 37:55–81. https://doi.org/10.1144/M37.13
Francis P, Oppenheimer C, Stevenson D (1993) Endogenous growth of persistently active volcanoes. Nature 366:554–557. https://doi.org/10.1038/366554a0
Harris AJL, Ripepe M (2007) Synergy of multiple geophysical approaches to unravel explosive eruption conduit and source dynamics – A case study from Stromboli. Geochemistry 67(1):1-35. https://doi.org/10.1016/j.chemer.2007.01.003
Galetto F, Reale D, Coppola D, Sansosti E, Pritchard ME (2025) The application of remote sensing data (SAR, thermal and optical) and geodetic modeling to investigate the volcanic activity at Semeru Volcano (Indonesia). J Geophys Res Solid Earth 130:e2025JB031428. https://doi.org/10.1029/2025JB031428
Ganci G, Vicari A, Cappello A, Del Negro C (2012) An emergent strategy for volcano hazard assessment: from thermal satellite monitoring to lava flow modeling. Remote Sens Environ 119:197–207. https://doi.org/10.1016/j.rse.2011.12.021
Giberti G, Jaupart C, Sartoris G (1992) Steady-state operation of Stromboli volcano, Italy: constraints on the feeding system. Bull Volcanol 54(7):535–541. https://doi.org/10.1007/BF00569938
Glaze L, Francis P, Rothery D (1989) Measuring thermal budgets of active volcanoes by satellite remote sensing. Nature 338:144–146. https://doi.org/10.1038/338144a0
Gurioli L, Colo L, Bollasina AJ, Harris AJL, Whittington A, Ripepe M (2014) Dynamics of Strombolian explosions: inferences from field and laboratory studies of erupted bombs from Stromboli volcano. J Geophys Res Solid Earth 119:319–345. https://doi.org/10.1002/2013JB010355
Harris AJL, Stevenson DS (1997) Magma budgets and steady-state activity of Vulcano and Stromboli volcanoes. Geophys Res Lett 24:1043–1046. https://doi.org/10.1029/97GL00861
Harris AJL, Flynn LP, Keszthelyi L, Mouginis-Mark PJ, Rowland SK, Resing JA (1998) Calculation of lava effusion rates from Landsat TM data. Bull Volcanol 60:52–71. https://doi.org/10.1007/s004450050216
Hornig-Kjarsgaard I, Keller J, Koberski U, Stadbauer E, Francalanci L, Lenhart R (1993) Geology, stratigraphy and volcanological evolution of the island of Stromboli, Aeolian arc, Italy. Acta Vulcanol 3:21–68
Insinga L, Voloschina M, Marianelli P, Bartolomeo E, Bertagnini A, Métrich N, Rotolo SG, Aiuppa A, Ripepe M, Pistolesi M (2025) Magma source, pre-eruptive dynamics and timescales of major explosions at Stromboli volcano (Italy). Bull Volcanol 87:75. https://doi.org/10.1007/s00445-025-01862-9
Justice CO, Giglio L, Korontzi S, Owens J, Morisette JT, Roy D, Descloitres J, Alleaume S, Petitcolin F, Kaufman Y (2002) The MODIS fire product. Remote Sens Environ 83:244–262. https://doi.org/10.1016/S0034-4257(02)00076-7
Kazahaya K, Shinohara H, Saito G (1994) Excessive degassing of Izu-Oshima volcano: magma convection in a conduit. Bull Volcanol 56(3):207–216. https://doi.org/10.1007/BF00279605
Kokelaar P, Romagnoli C (1995) Sector collapse, sedimentation and clast population evolution at an active island-arc volcano: Stromboli, Italy. Bull Volcanol 57(4):240–262. https://doi.org/10.1007/BF00265424
La Felice S, Landi P (2011) The 2009 paroxysmal explosions at Stromboli (Italy): magma mixing and eruption dynamics. Bull Volcanol 73:1147–1154. https://doi.org/10.1007/s00445-011-0502-z
Laiolo M, Massimetti F, Cigolini C, Ripepe M, Coppola D (2018) Long-term eruptive trends from space-based thermal and emissions: a comparative analysis of Stromboli, Batu Tara and Tinakula volcanoes. Bull Volcanol 80:9. https://doi.org/10.1007/s00445-018-1242-0
Laiolo M, Ripepe M, Cigolini C, Coppola D, Della Schiava M, Genco R, Innocenti L, Lacanna G, Marchetti E, Massimetti F, Silengo MC (2019) Space- and ground-based geophysical data tracking of magma migration in shallow feeding system of Mount Etna volcano. Remote Sens 11:1182. https://doi.org/10.3390/rs11101182
Laiolo M, Delle Donne D, Coppola D, Bitetto M, Cigolini C, Della Schiava M, Innocenti L, Lacanna G, La Monica FP, Massimetti F, Pistolesi M, Silengo MC, Aiuppa A, Ripepe M (2022) Shallow magma dynamics at open-vent volcanoes tracked by coupled thermal and SO2 observations. Earth Planet Sci Lett 594:117726. https://doi.org/10.1016/j.epsl.2022.117726
Landi P, Corsaro RA, Francalanci L, Civetta L, Miraglia L, Pompilio M, Tesoro R (2009) Magma dynamics during the 2007 Stromboli eruption (Aeolian Islands, Italy): mineralogical, geochemical and isotopic data. J Volcanol Geoth Res 182(3–4):255–268. https://doi.org/10.1016/j.jvolgeores.2008.11.010
Lo Bue Trisciuzzi G, Aiuppa A, Salerno G, Bitetto M, Curcio L, Innocenti L, Lacanna G, Lages JPN, Lo Forte FM, Maugeri SR, Murè F, Principato P, Ripepe M, Vitale A, Delle Donne D (2024) Improved volcanic SO_2 flux records from integrated scanning-DOAS and UV Camera observations. J Volcanol Geotherm Res 455. https://doi.org/10.1016/j.jvolgeores.2024.108207
Marsella M, Baldi P, Coltelli M, Fabris M (2012) The morphological evolution of the Sciara del Fuoco since 1868: reconstructing the effusive activity at Stromboli volcano. Bull Volcanol 74:231–248. https://doi.org/10.1007/s00445-011-0516-6
Massimetti F, Laiolo M, Aiuppa A, Aveni S, Bitetto M, Campus A, Coltelli M, Cristaldi A, Delle Donne D, Innocenti L, Lacanna G, Pistolesi M, Privitera E, Ripepe M, Salerno G, Coppola D (2024) Thermal emissions of active craters at Stromboli volcano:

spatio-temporal insights from 10 years of satellite observations. J Geophys Res Solid Earth 129:9. https://doi.org/10.1029/2024JB029143

Métrich N, Bertagnini A, Landi P, Rosi M (2001) Crystallization driven by decompression and water loss at Stromboli volcano (Aeolian Islands, Italy). J Petrol 42:1471–1490. https://doi.org/10.1093/petrology/42.8.1471

Métrich N, Bertagnini A, Landi P, Rosi M, Belhadj O (2005) Triggering mechanism at the origin of paroxysms at Stromboli (Aeolian archipelago, Italy): the 5 April 2003 eruption. Geophys Res Lett 32(10):L10305. https://doi.org/10.1029/2004GL022257

Métrich N, Bertagnini A, Di Muro A (2010) Conditions of magma storage, degassing and ascent at Stromboli: new insights into the volcano plumbing system with inferences on the eruptive dynamics. J Petrol 51:603–626. https://doi.org/10.1093/petrology/egp083

Métrich N, Bertagnini A, Pistolesi M (2021) Paroxysms at Stromboli volcano (Italy): source, genesis and dynamics. Front Earth Sci 9:593339. https://doi.org/10.3389/feart.2021.593339

Naismith A, Watson I, Quinillo CC, Chigna G, Escobar-Wolf R, Coppola D, Chun C (2019) Eruption frequency patterns through time for the current (1999–2018) activity cycle at Volcán de Fuego derived from remote sensing data: evidence for an accelerating cycle of explosive paroxysms and potential implications of eruptive activity. J Volcanol Geotherm Res 371:206–219. https://doi.org/10.1016/j.jvolgeores.2019.01.001

Newhall CG, Costa F, Ratdomopurbo A, Venezky DY, Widiwijayanti C, Win NTZ, Tan K, Fajiculay E (2017) WOVOdat – an online, growing library of worldwide volcanic unrest. J Volcanol Geotherm Res 345:184–199. https://doi.org/10.1016/j.jvolgeores.2017.08.003

Oppenheimer C, Rothery DA, Pieri DC, Abrams MJ, Carrere V (1993a) Analysis of airborne visible/infrared imaging spectrometer (AVTRIS) data of volcanic hot spots. Int J Remote Sens 14(16):2919–2934. https://doi.org/10.1080/01431169308904411

Oppenheimer C, Rothery DA, Francis PW (1993b) Thermal distributions at fumarole fields – implications for infrared remote-sensing of active volcanos. J Volcanol Geotherm Res 55(1–2):97–115. https://doi.org/10.1016/0377-0273(93)90092-6

Pallister J, McNutt SR (2015) Synthesis of volcano monitoring. In: Sigurdsson H (ed) The Encyclopedia of Volcanoes, 2nd edn. Academic Press, Cambridge, MA, pp 1151–1171. https://doi.org/10.1016/B978-0-12-385938-9.00066-3

Palma JL, Blake S, Calder ES (2011) Constraints on the rates of degassing and convection in basaltic open-vent volcanoes. Geochem Geophys Geosyst. https://doi.org/10.1029/2011GC003715

Patrick MR, Harris AJL, Ripepe M, Dehn J, Rothery DA, Calvari S (2007) Strombolian explosive styles and source conditions: insights from thermal (FLIR) video. Bull Volcanol 69(7):769–784. https://doi.org/10.1007/s00445-006-0107-0

Phillipson G, Sobradelo R, Gottsmann J (2013) Global volcanic unrest in the 21st century: an analysis of the first decade. J Volcanol Geotherm Res 264:183–196. https://doi.org/10.1016/j.jvolgeores.2013.08.004

Pioli L, Pistolesi M, Rosi M (2014) Transient explosions at open-vent volcanoes: the case of Stromboli (Italy). Geology 42(10):863–866. https://doi.org/10.1130/G35844.1

Pistolesi M, Delle Donne D, Pioli L, Rosi M, Ripepe M (2011) The 15 March 2007 explosive crisis at Stromboli volcano, Italy: assessing physical parameters through a multidisciplinary approach. J Geophys Res Solid Earth 116:1–18. https://doi.org/10.1029/2011JB008527

Poland MP, de Zeeuw-van Dalfsen E (2020) Volcano geodesy: A critical tool for assessing the state of volcanoes and their potential for hazardous eruptive activity. In: Wadge G, Sparks RSJ, Gottsmann J (eds) Forecasting and Planning for Volcanic Hazards, Risks, and Disasters. Elsevier, Amsterdam, pp 75–115. https://doi.org/10.1016/B978-0-12-818082-2.00003-2

Ripepe M, Harris AJL, Carniel R (2002) Thermal, seismic and infrasonic evidences of variable degassing rates at Stromboli volcano. J Volcanol Geotherm Res 118(3–4):285–297. https://doi.org/10.1016/S0377-0273(02)00298-6

Ripepe M, Marchetti E, Ulivieri G, Harris AJL, Dehn J, Burton M, Caltabiano T, Salerno G (2005) Effusive to explosive transition during the 2003 eruption of Stromboli volcano. Geology 33:341–344. https://doi.org/10.1130/G21173.1

Ripepe M, Delle Donne D, Lacanna G, Marchetti E, Ulivieri G (2009) The onset of the 2007 Stromboli effusive eruption recorded by an integrated geophysical network. J Volcanol Geotherm Res 182(3–4):131–136. https://doi.org/10.1016/j.jvolgeores.2009.02.011

Ripepe M, Delle Donne D, Genco R, Maggio G, Pistolesi M, Marchetti E, Lacanna G, Ulivieri G, Poggi P (2015) Volcano seismicity and ground deformation unveil the gravity-driven magma discharge dynamics of a volcanic eruption. Nat Commun 6:6998. https://doi.org/10.1038/ncomms7998

Ripepe M, Pistolesi M, Coppola D, Delle Donne D, Genco R, Lacanna G, Laiolo M, Marchetti E, Ulivieri G, Valade S (2017) Forecasting effusive dynamics and decompression rates by magmastatic model at open-vent volcanoes. Sci Rep 7:3885. https://doi.org/10.1038/s41598-017-03833-3

Ripepe M, Lacanna G, Pistolesi M, Silengo MC, Aiuppa A, Laiolo M, Massimetti F, Innocenti L, Della Schiava M, Bitetto M, La Monica FP, Nishimura T, Rosi M, Mangione D, Ricciardi A, Genco R, Coppola D, Marchetti E, Delle Donne D (2021) Ground deformation reveals the scale-invariant conduit dynamics driving explosive basaltic eruptions. Nat Commun 12:1683. https://doi.org/10.1038/s41467-021-2172

Ripepe M, Delle Donne D, Harris AJL, Marchetti E, Ulivieri G (2008) Dynamics of Strombolian activity. In: Calvari S, Inguaggiato S, Puglisi G, Ripepe M, Rosi M (eds) Learning from Stromboli: an integrated study of the 2002–2003 eruption. Geophysical Monograph Series, vol 182. American Geophysical Union, Washington DC, pp 39–48. https://doi.org/10.1029/182GM05

Rose WI, Palma JL, Delgado Granados H, Varley N (2013) Open-vent volcanism and related hazards: overview. Geol Soc Am Spec Pap 498:vii–xiii. https://doi.org/10.1130/9780813724980

Rosi M, Bertagnini A, Landi P (2000) Onset of the persistent activity at Stromboli volcano (Italy). Bull Volcanol 62:294–300. https://doi.org/10.1007/s004450000098

Rosi M, Pistolesi M, Bertagnini A, Landi P, Pompilio M, Di Roberto A (2013) Stromboli volcano, Aeolian Islands (Italy): present eruptive activity and hazards. In: Keller J (ed) Geol Soc Lond Mem 37:473–490. https://doi.org/10.1144/M37.14

Shinohara H (2008) Excess degassing from volcanoes and its role on eruptive and intrusive activity. Rev Geophys. https://doi.org/10.1029/2007RG000244

Shreve T, Grandin R, Boichu M, Garaebiti E, Moussallam Y, Ballu V, Delgado F, Leclerc F, Vallée M, Henriot N, Cevuard S, Tari D, Lebellegard P, Pelletier B (2019) From prodigious volcanic degassing to caldera subsidence and quiescence at Ambrym (Vanuatu): the influence of regional tectonics. Sci Rep 9:18868. https://doi.org/10.1038/s41598-019-55141-7

Sparks RSJ, Biggs J, Neuberg JW (2012) Monitoring volcanoes. Science 335:1310–1311. https://doi.org/10.1126/science.1219485

Stevenson DS, Blake S (1998) Modelling the dynamics and thermodynamics of volcanic degassing. Bull Volcanol 60:307–317. https://doi.org/10.1007/s004450050234

Thompson JO, Williams DB, Ramsey MS (2023) The expectations and prospects for quantitative volcanology in the upcoming Surface Biology and Geology (SBG) era. Earth Space Sci 10:e2022EA002817. https://doi.org/10.1029/2022EA002817

Tibaldi A (2001) Multiple sector collapses at Stromboli volcano, Italy: how they work. Bull Volcanol 63:112–125. https://doi.org/10.1007/s004450100

Valade S, Lacanna G, Coppola D, Laiolo M, Pistolesi M, Delle Donne D, Genco R, Marchetti E, Ulivieri G, Allocca C, Cigolini C, Nishimura T, Poggi P, Ripepe M (2016) Tracking dynamics of magma migration in open-conduit systems. Bull Volcanol 78:11. https://doi.org/10.1007/s00445-016-1072-x

Vasconez FJ, Hidalgo S, Battaglia J, Hernandez S, Bernard B, Coppola D, Valade S, Ramón P, Arellano S, Liorzon C, Almeida M, Ortiz M, Córdova J, Vásconez Müller A (2022) Linking ground-based data and satellite monitoring to understand the last two decades of eruptive activity at Sangay volcano. Ecuador. Bull Volcanol 84:49. https://doi.org/10.1007/s00445-022-01560-w

Vergniolle S, Métrich N (2021) Open-vent volcanoes: a preface to the special issue. Bull Volcanol 83:29. https://doi.org/10.1007/s00445-021-01454-3

Voloschina M, Métrich N, Bertagnini A, Marianelli P, Aiuppa A, Ripepe M, Pistolesi M (2023) Explosive eruptions at Stromboli volcano (Italy): a comprehensive geochemical view on magma sources and intensity range. Bull Volcanol 85(6):1–21. https://doi.org/10.1007/s00445-023-01647-y

Wadge G (1982) Steady state volcanism: evidence from eruption histories of polygenetic volcanoes. J Geophys Res 87(B5):4035–4049. https://doi.org/10.1029/JB087iB05p04035

Wooster MJ, Zhukov B, Oertel D (2003) Fire radiative energy for quantitative study of biomass burning: derivation from the BIRD experimental satellite and comparison to MODIS fire products. Rem Sens Environm 86:83–107. https://doi.org/10.1016/S0034-4257(03)00070-1

Wright R, Flynn L, Garbeil H, Harris AJL, Pilger E (2002) Automated volcanic 1435 eruption detection using MODIS. Remote Sens Environ 82:135–155

Authors and Affiliations

Marco Laiolo[1,2] · Diego Coppola[1,2] · Simone Aveni[1,3] · Adele Campus[1] · Francesco Massimetti[4] · Alessandro Aiuppa[5] · Lorenzo Innocenti[6] · Giorgio Lacanna[6] · Giovanni Lo Bue Trisciuzzi[5] · Marco Pistolesi[7] · Maurizio Ripepe[6] · Marija Voloschina[7]

✉ Marco Laiolo
marco.laiolo@unito.it

Diego Coppola
diego.coppola@unito.it

Simone Aveni
simonesalvatore.aveni@unito.it

Adele Campus
adele.campus@unito.it

Francesco Massimetti
francesco.massimetti@igeofisica.unam.mx

Alessandro Aiuppa
alessandro.aiuppa@unipa.it

Lorenzo Innocenti
lorenzo.innocenti@unifi.it

Giorgio Lacanna
giorgio.lacanna@unifi.it

Giovanni Lo Bue Trisciuzzi
giovanni.lobuetrisciuzzi@unipa.it

Marco Pistolesi
marco.pistolesi@unipi.it

Maurizio Ripepe
maurizio.ripepe@unifi.it

Marija Voloschina
marija.voloschina@dst.unipi.it

[1] Dipartimento Di Scienze Della Terra, Università Di Torino, Via Valperga Caluso, 35, 10125 Turin, Italy

[2] Centro Interdipartimentale Sui Rischi Naturali in Ambiente Montano E Collinare (NATRISK), Università Degli Studi Di Torino, Largo Paolo Braccini 2, 10095 Grugliasco, Turin, Italy

[3] Dipartimento Di Ingegneria Civile Edile E Ambientale, Università Di Roma Sapienza, Piazzale Aldo Moro 5, 00185 Rome, Italy

[4] Instituto de Geofisica, Universidad Autonoma de Mexico, UNAM, Circuito de la Investigación Científica S/N, C.U., 04150 Coyoacán, CDMX, Mexico

[5] Dipartimento Di Scienze Della Terra E del Mare, DiSTeM, Università Di Palermo, Via Archirafi, 22, 90123 Palermo, Italy

[6] Dipartimento Di Scienze Della Terra, Università Di Firenze, Via La Pira, 4, 50121 Florence, Italy

[7] Dipartimento Di Scienze Della Terra, Università Di Pisa, Pisa, Via S. Maria 53, 56126 Pisa, Italy